BMC Plant Biology

RESEARCH

Open Access

Transcriptomic and proteomic-based analysis of the mechanisms by which drought and salt stresses affect the quality of *Isatidis Folium*

Zhiying Wang[1,2†], Baorui Cao[1,2,3†], Jinxin Du[2], Tingting Deng[3], Ruyu Wang[2], Yiwei Chen[2], Xue Li[2], Jialei Fu[4], Jingxiang Pang[2], Meina Yang[1,2*†] and Jinxiang Han[1,2†]

Abstract

Isatidis Folium, derived from the dried leaves of *Isatis indigotica* Fort., has been used for centuries as a traditional Chinese herb with antibacterial and antiviral properties. However, heterogeneity in cultivation conditions and climatic variations poses challenges to accurately and effectively evaluate its quality. Current quality control methods cannot provide a comprehensive and effective identification of herbal quality and preparation efficacy. This study aimed to investigate the impact of different environmental factors on the biosynthesis and accumulation of medicinal components and identify biomarker genes and functional proteins associated with abiotic stress responses of *Isatis indigotica* Fort. We proposed evaluating the quality of *Isatidis Folium* based on multi-component quantitative analysis and integrating transcriptomic, proteomic, and physiological indicators to elucidate the mechanisms of herbal quality variation. The results revealed that abiotic stress conditions significantly altered the levels of bioactive constituents, physiological indices, and specific genes and proteins. Notably, biological pathways such as porphyrin metabolism, photosynthesis, and carbon fixation by photosynthetic organisms were implicated in phototoxicity within the photosystem under abiotic stresses. Biological pathways related to indole metabolism, specifically phenylalanine, tyrosine, and tryptophan synthesis, tryptophan metabolism, and indole alkaloid synthesis, were recognized as critical regulatory networks modulating indole alkaloid content. Candidate biomarkers such as *HemB*, *PsbB*, *RBS2*, *RIBA2*, *TRPA*, and *TRPB* were identified as potential factors of quality deterioration under adverse conditions. Based on the integration of chemical analysis and multi-omics techniques, a new hierarchical quality control scenario for *Isatidis Folium* was finally proposed, providing a research foundation for the innovation-driven development of traditional Chinese medicine.

Keywords *Isatidis Folium*, Stress, Herbal quality, Multi-component quantitative analysis, Transcriptomic, Proteomic, Biological mechanism

†Zhiying Wang and Baorui Cao contributed equally to this paper and share the first authorship..

†Meina Yang and Jinxiang Han contributed equally to this paper and share the last authorship..

*Correspondence:
Meina Yang
xz19560659193@163.com
Full list of author information is available at the end of the article

Introduction

The cruciferous plant *Isatis indigotica* Fort. (*I. indigotica*) [Brassicaceae] is predominantly cultivated in the Yellow River basin north of the Yangtze River [1]. It is cold-resistant, warmth-favoring, and moderately drought-tolerant but vulnerable to waterlogging [2]. As a medicinal plant, its dried leaves are the traditional Chinese herb *Isatidis Folium*, which has been listed in the Chinese Pharmacopoeia since 1985. *Isatidis Folium* is believed to clear heat and toxic substances, cool blood, and eliminate spots, and it has been widely used in Eastern countries for centuries. It has been proven to possess various pharmacological activities, such as antibacterial, anti-inflammatory, anti-endotoxin, and anti-cancer effects [3]. Preclinical studies indicate that *Isatidis Folium* extracts inhibit RNA/DNA viruses (e.g., influenza A, adenovirus) in vitro and reduce viral titers in murine models [4]. Additionally, these extracts exhibit anti-inflammatory and antioxidant activities by suppressing pro-inflammatory cytokines (TNF-α and IL-6) and reactive oxygen species (ROS) production in macrophage models [1]. Clinically, *Isatidis Folium* is commonly used to alleviate symptoms of colds, fevers, sore throats, viral hepatitis, and epidemic encephalitis B [5, 6]. Phytochemical analyses reveal that *Isatidis Folium* primarily contains bioactive constituents such as alkaloids [7–9], flavonoids [10, 11], organic acids [12–14], and polysaccharides [15, 16]. Among these, indole alkaloids are the most important class of bioactive constituents in *Isatidis Folium* [17], and indigo and indirubin are the most bioactive and iconic indole alkaloid ingredients; their contents are important factors affecting the quality of *Isatidis Folium*. Indigo is the main active ingredient of *Isatidis Folium* [1] and has been proven to exert liver-protective and antibiotic functions [18]. Indirubin has been shown to have excellent antibacterial, anti-inflammatory, anti-leukemic, and immune-enhancing activities [19, 20].

The quality of *Isatidis Folium* is difficult to control due to the influence of several factors, including its origin, germplasm, growing environment, and harvesting season. The use of artificial organic pesticides and fertilizers has increased the levels of organic phosphorus, organic nitrogen, heavy metal ions, microorganisms, and other residues in *Isatidis Folium* [21]. Such contamination can compromise herbal quality, potentially diminishing its clinical efficacy. At present, soil salinization and climatic drought are significant issues, and the two most prevalent abiotic stresses affecting herbaceous plants are salt and drought stresses. Since the factors influencing the quality of *Isatidis Folium* are highly complex, the current quality control system is inadequate. Its quality control and material basis remain key issues. According to the Chinese Pharmacopoeia 2020, the indirubin content of *Isatidis Folium* should be determined using high-performance liquid chromatography (HPLC) as a quality evaluation method [2]. Currently, reversed-phase high-performance liquid chromatography (RP-HPLC) is the main method used to quantify the major bioactive constituents in *Isatidis Folium* [22]. In terms of the overall quality control of the chemical components of *Isatidis Folium*, Wang Yin [23] utilized high-performance capillary electrophoresis to differentiate between populations of *Isatidis Folium.* Although some studies have explored holistic quality control of its chemical components, most current methods focus on only a few ingredients. Quality assessment tends to rely on single indicators, making accurate evaluation of the quality of *Isatidis Folium* more difficult [24]. Relevant research is scattered, failing to form a unified and recognized quality control method and system. This has resulted in inconsistent herbal quality in the market, and related compound formulas and traditional Chinese medicinal preparations struggle to meet quality standards, leading to suboptimal clinical effects [25]. As a result, this situation has posed significant challenges to the quality control of *Isatidis Folium* and the development of modern Chinese medicine [26, 27]. Consequently, these challenges hinder the quality control of *Isatidis Folium* and establish a quality evaluation method that is consistent with the holistic view of traditional Chinese medicine and is tailored to the specific characteristics of *Isatidis Folium*. Such an approach would help improve the quality evaluation system for this Chinese herb [1].

Transcriptomic and proteomic sequencing are widely used and highly efficient molecular biology analysis techniques that can reflect both gene and protein expression levels of organisms at specific developmental stages or under certain physiological conditions. These technologies have played crucial roles in understanding how plants respond to adversity [28–30]. Notably, existing literature has elucidated how key genes or proteins regulated by external environmental stimuli mediate the biosynthesis of secondary metabolites or modulate bioactive constituent levels in herbal plants. These findings provide valuable insights for genetic studies, quality breeding, and the determination of optimal cultivation conditions [31–33]. However, current studies on abiotic stress responses in *I. indigotica* mainly focus on the levels of seed germination, seedling growth, and physiological indices [34–36], while little consideration has been given to the accumulation of bioactive constituents and the quality of its leaves. More importantly, the intrinsic mechanisms through which abiotic stresses regulate the quality of *Isatidis Folium* remain poorly understood.

This study aims to provide a comprehensive understanding of the changes in physiological status and the

accumulation of bioactive constituents of *I. indigotica* leaves under stress conditions and to elucidate the intrinsic regulatory mechanisms of how adverse stresses affect the quality of *Isatidis Folium* from multiple perspectives. Investigating the effects of environmental ecological factors on the production and accumulation of medicinal composition in Chinese herbs and screening for key signature genes and functional proteins will help us to accurately understand the causes of changes in herbal quality under different stress conditions. Therefore, we established two abiotic stresses for *I. indigotica*: drought stress and salt stress. Ultrahigh performance liquid chromatography (UPLC)-based determination of multi-component content was integrated to evaluate the quality of *Isatidis Folium* under different stress conditions. The physiological status of *I. indigotica* leaves was accurately identified by testing physiological indicators. The biological pathways and regulatory networks underlying stress-induced changes in the quality of *Isatidis Folium* were explored by integrating transcriptomic and proteomic analyses. Finally, we propose a concept of hierarchical quality control of *Isatidis Folium* at the level of chemical analyses and multi-omics techniques.

Materials and methods

Herbal cultivation and stress treatments

Cultivation of I. indigotica

I. indigotica seeds were purchased from Bozhou Changnong Chinese Medicinal Materials Planting Co., Ltd., and identified by Fu Jialei. *I. indigotica* was planted in boxes (0.4 m × 1.2 m × 0.5 m) in the herbal garden of Shandong First Medical University (36° 8′ 6" N, 116° 8′ 6" E, Jinan, Shandong Province, China) on 20 August 2022. Before sowing, the soil was turned to a depth of 30 cm, and sheep manure was applied as a basal fertilizer. Trenches (3–4 cm deep) were prepared for sowing, with plant spacing of 5–8 cm and row spacing of 15 cm. The same insulated sheds were constructed around all the boxes. No shading treatment was applied during cultivation, but 24-h ventilation was maintained. Salt and drought stress treatments were applied separately, with each condition maintained as an independent experimental group. The technical specifications for cultivation, collection, storage, and primary processing were carried out according to the Law of the People's Republic of China on Traditional Chinese Medicine and other relevant regulations [37].

Drought stress treatment

This experiment was conducted from 1 September to 1 November. After seed emergence, two boxes of *I. indigotica* exhibiting uniform growth vigor were selected for further cultivation. Each box contained approximately 50 plants. Two irrigation treatments were established: the control group (adequate water supply), with a soil water content of 70%–90% through thrice-weekly irrigation with 3 L of well water. The drought stress group, with a soil relative water content of 30%–50% through biweekly irrigation with 1 L of water. To maintain the soil water content within the set range, daily evaporation was compensated for by measuring the soil moisture each evening using the gravimetric method [38] and adjusting the water application accordingly. This approach ensured that all the treatments adhered to their designated moisture conditions. The drought stress treatment lasted for two months.

Salt stress treatment

After sowing, *I. indigotica* was cultivated under the same growing conditions. Twenty days after seedling emergence, two boxes of uniformly vigorous *I. indigotica* (approximately 50 plants per box after thinning) were selected for salt stress treatment. Two different concentration gradients of sodium chloride, 0 mmol/L (the control group) and 180 mmol/L (the stress group), were established for the salt stress treatment. To prevent osmotic stress, the salinity was gradually increased, starting at 1/3 of the predetermined concentration for the first stress, 2/3 for the second stress, and reaching the full predetermined concentration for the third stress. Salt stress was applied once a week for one month, with each application delivering a saline solution equivalent to twice the soil water-holding capacity [39]. Daily soil samples from each treatment group were oven-dried, and soil salinity was determined using the electrical conductivity method [40] to maintain target gradient levels throughout the stress period.

Multi-component quantitative analysis based on UPLC

Sample preparation for content determination

After the fresh *I. indigotica* leaves were collected, they were washed with double distilled water, blotted with absorbent paper, and dried in a drying box (Shanghai Huitai Instrument Manufacturing Co., Ltd) at 60 °C for 24 h. The dried leaves were then ground using an 800C multifunction grinder (Dongguan Fanta Electrical Co., Ltd.) and sieved through a 65-mesh Chinese medicine sieve (0.212 mm aperture). Finally, the samples were placed in centrifuge tubes and stored in a cool and dry place.

A total of 3 g of dried *Isatidis Folium* powder was accurately weighed and transferred to a flask. 50 mL of chloroform was added, and the mixture was thoroughly shaken and weighed. The sample was then heated and refluxed for 30 min, cooled, and reweighed, and chloroform was added to compensate for the weight loss. The

mixed solution was then thoroughly shaken, filtered, and concentrated to dryness. An appropriate amount of methanol-chloroform mixture (8:2, v/v) was added to dissolve the residue. The solution was then transferred to a 10 mL volumetric flask, diluted to the mark with the same solvent, and mixed thoroughly to obtain the test solution of *Isatidis Folium*.

Calibration standards and UPLC analysis

The UPLC analysis was performed on a Waters Acquity ultra-high performance liquid chromatograph (Waters, Milford, MA, USA) equipped with an ACQUITY UPLC sample organizer, a chromatographic column manager, a column temperature box with heating and cooling functions, a binary solvent manager and sample manager, a photodiode array, and an evaporative light scattering detector. The chromatographic analysis was performed using an ACQUITY UPLC BEH C_{18} column (150 mm × 2.1 mm × 1.7 μm) with a mobile phase of 0.1% phosphoric acid solution (A)—methanol (B). A gradient elution was used (the procedure is shown in Table 1). Before testing, the mobile phase was degassed by ultrasonication in a PL-S40 digital ultrasonic cleaner (Dongguan Kangshijie Ultrasonic Technology Co., Ltd.) for 15 min. The detection time was 35 min, the injection volume was 10 μL, and the flow rate was 0.3 mL/min. The column temperature was maintained at 35 °C, and the sample cell temperature was set at 25 °C.

High-purity controls (≥98%) were used for calibration, including 4-hydroxyquinazoline, syringic acid, tryptanthrin, indigo, and indirubin, all purchased from Shanghai Yuanye Biotechnology Co. Standard curves were generated using the 6-point gradient concentration method. The mixed standard solution was precisely prepared to perform the precision test according to the above chromatographic conditions for 6 consecutive injections. The stability test was performed by storing the mixed standard solution at room temperature for 0, 2, 4, 8, 12, and 24 h. Repeatedly, six test solutions were prepared separately for the reproducibility test. Three portions of the known content of 0.5 g of *Isatidis Folium* were accurately weighed and placed in centrifuge tubes. Appropriate amounts of the mixed standard solution were added to these tubes (the amounts added were 50%, 100%, and 150% of the sample content, respectively). Six samples were prepared and tested in parallel for each group. The average recovery of each component was calculated using the following equation:

$$P = \left(\frac{C_1 - C_2}{C_3} \right) \times 100\% \quad (1)$$

P is the average recovery (%), C_1 is the total content measured after the addition of the standard, C_2 is the content of the sample, and C_3 is the content of the added standard.

Table 1 Gradient elution program

Time (min)	A (%)	B (%)	Time (min)	A (%)	B (%)
0	75	25	18.5	30	70
3.5	74	26	25	12	88
5	65	35	26	12	88
6	65	35	26.01	75	25
10	55	45	33	75	25

Determination of physiological indicators

Fresh samples were collected and processed, and the content of photosynthetic pigments was determined using a U-3900H UV/VIS spectrophotometer (Hitachi High-Tech, Tokyo, Japan). The fresh *I. indigotica* leaves were submerged in a 1:1 (v/v) mixture of 80% acetone and anhydrous ethanol. The samples were then kept in the dark until the leaves had completely decolored, after which the extract was extracted. The acetone–ethanol mixture was used as a reference for colorimetry via ultraviolet spectrophotometry, and the absorbance values were determined at 474, 642, and 665 nm. The chlorophyll and carotenoid contents were determined according to Huang [41] and were calculated using the corresponding equations. The net photosynthetic rate was measured using a Chlorolab-2 liquid-phase oxygen electrode (Hansatech Oxygraph, UK). The relative electrical conductivity (REC) was measured using a DDS-11A conductivity meter (Shanghai Yitian Scientific Instrument Co., Ltd). Three replicate experiments were performed for each treatment. The REC was calculated using the following equation:

$$E = \frac{E_2 - E_1}{E_3 - E_1} \quad (2)$$

E_1, E_2, and E_3 represent the conductivities of the double distilled water, samples, and samples after boiling in a water bath, respectively.

Transcriptomic analysis based on RNA sequencing technology

RNA extraction and library construction

Transcriptome sequencing was performed by Shanghai Bioprofile Technology Company, Ltd. Total RNA was extracted using Trizol reagent (Invitrogen Life Technologies). Sequencing library construction was performed using the TruSeq RNA Sample Preparation Kit (Illumina, San Diego, CA, USA). After library construction, the products were purified using the AMPure XP system,

and the DNA was quantified using the Bioanalyzer 2100 system.

RNA sequencing

RNA sequencing was performed on the NovaSeq 6000 platform (Illumina, San Diego, CA, USA). The sequencing data were filtered for high-quality sequences using Cutadapt v1.15 software. In the absence of a transcriptome sequencing project for the *I. indigotica* reference genome, a Montage Clear Read was performed on the transcripts using Trinity v2.5.1 software to obtain transcript sequence files. The longest transcript of each gene was extracted as a representative sequence of that gene, called a "unigene".

Transcriptomic data analysis

The nonredundant protein sequence (NR), GO, KEGG, evolutionary genealogy of Genes: Non-supervised Orthologous Groups (eggNOG), SwissProt, and Pfam databases were used to annotate the gene functions of these unigenes. For differential expression analysis, RSEM 1.2.31 was used to compare read counts for each gene as the raw expression of the gene, and FPKM was used to normalize the expression. Differentially expressed genes (DEGs) were screened using the expression difference multiplicity $|\log2FoldChange| > 1$ and $P < 0.05$ as conditions and analyzed via DESeq 1.30.0. All genes were mapped to terms in the GO database, and the number of DEGs associated with each term was calculated. GO enrichment analysis of DEGs was performed via topGO, and P values were calculated using the hypergeometric distribution method (the criterion for significant enrichment was $P < 0.05$). GO entries significantly enriched in DEGs were screened based on the P values to identify the main biological functions associated with the DEGs. KEGG pathway enrichment analysis of DEGs with $P < 0.05$ was performed using ClusterProfiler 3.4.4.

Proteomic analysis based on TMT technology

Protein extraction, quantification, and enzymatic hydrolysis

A sample of 0.1 g of fresh *Isatidis Folium* was precisely weighed, ground with liquid nitrogen, and mixed with 200 μL of SDT lysate (4% SDS, 100 mM DTT, 150 mM Tris–HCl, pH 8.0). The mixture was placed in a water bath at 95 °C for 3 min, followed by sonication for 2 min. The mixture was then centrifuged at 4 °C for 20 min at 16,000 × g. The protein content was measured via the Bradford assay [42], and enzymatic hydrolysis was performed using the filter-aided sample preparation method proposed by Wisniewski [43].

TMT peptide labeling and classification

An appropriate amount of peptide was dissolved in 100 μL of 0.05 M tetraethylammonium bromide solution (pH 8.5). The TMT reagent was dissolved in 41 μL of anhydrous acetonitrile. The two were mixed and incubated at room temperature for 1 h. 8 μL of 5% hydroxylamine was added and incubated for 15 min to quench the reaction. Aliquots of each group of labeled peptides were mixed and lyophilized. The TMT-labeled peptide mixture was separated on an Agilent 1290 HPLC with a Waters XBridge BEH 130C column (C_{18}, 2.1 mm × 150 mm × 3.5 μm). The buffers were 10 mM ammonium formate and 10 mM ammonium formate in 90% acetonitrile, and the pH was adjusted to 10.0 with ammonium hydroxide. The flow rate was set at 0.3 mL/min. A total of 15 fractions were eventually collected for each mixture. The samples were then dried and resolubilized with 0.1% FA.

Liquid chromatography-mass spectrometer (LC–MS)/MS analysis

An appropriate amount of peptide sample was taken and chromatographically separated using an Easy nLC 1200 chromatography system. The buffers used were A (0.1% formic acid aqueous solution) and B (a mixture of 0.1% formic acid, 95% acetonitrile, and water), and solution A was used to equilibrate the column. The sample was first injected into a trap column (C_{18}, 100 μm × 20 mm × 5 μm) and then eluted through a chromatographic column (C_{18}, 75 μm × 150 mm × 3 μm). The gradient elution program was as follows: 0–2 min, 2% B–8% B; 2–71 min, 8% B–28% B; 71–79 min, 28% B–40% B; 79–81 min, 40% B–100% B; and 81–90 min, 100% B. The flow rate was set at 300 nL/min. At the end of the gradient elution, a Q Exactive HF-X mass spectrometer was used for data-dependent acquisition mode analysis.

Proteomic data analysis

Database searches of the raw data files were performed using Proteome Discoverer 2.4 software and the Sequest HT search engine. The enzyme used was trypsin, the maximum cleavage site was 2, the tolerance for the main search peptide was 10 ppm, the fixed modifications were aminomethyl (C), TMTpro (K), and TMTpro (N-terminal peptide), the variable modifications were oxidation (M) and acetylation (N-terminal peptide), the database was "*Isatis indigotica* Fortune-Unigene.fa.transdecoder.pep.fasta", the PSM FDR was ≤ 0.01, and the protein FDR was ≤ 0.01.

The above data were bioinformatically analyzed using Perseus, Microsoft Excel, and the R package. Proteins with a critical value of > 1.20 or < 0.83 with $P < 0.05$ for

the fold change ratio were identified as differentially expressed proteins (DEPs), and the DEPs were then analyzed by hierarchical clustering. Information was extracted from UniProtKB/Swish-Prot, Kyoto Encyclopedia of Genes and Genomes (KEGG), and Gene Ontology (GO) to annotate the sequences. GO and KEGG enrichment analyses were performed using Fisher's exact test, and entries with $P < 0.05$ were considered statistically significant and corrected for FDR for multiple trials.

Quantitative real-time polymerase chain reaction (qPCR) validation of the DEGs

To validate the accuracy of the RNA sequencing expression data, ten key DEGs were selected for qRT−PCR via the Roche Light Cycler 480 II real-time fluorescence quantitative PCR system (Bio-Rad, Berkeley, CA, USA). Total RNA was extracted from the fresh *I. indigotica* leaves via the E.Z.N.A.® Plant RNA Kit (Omega Biotek, Norcross, GA, USA). The extracted RNA was then reverse transcribed into cDNA using SPARK script II reverse transcriptase, with *GAPDH* serving as an internal reference gene. Relative expression levels were determined using SYBR Green II. Three biological replicates were performed for each group of samples, and four to five technical replicates were performed for each sample. All primer information is shown in Table 2.

Data statistical analysis

Statistical analyses and data visualization were performed using GraphPad Prism 9.5.0 (GraphPad Software, La Jolla, CA, USA; www.graphpad.com). Significant differences in data from samples under different stress conditions were evaluated using a two-tailed unpaired Student's t-test. In all the statistical tests, $P \leq 0.05$ was considered statistically significant. The results of statistical analyses were presented as mean ± standard deviation (SD) based on at least three biological replicates.

Results

Phenotypic responses of *I. indigotica* leaves to abiotic stresses

When plants encounter environmental stresses, the most observable primary effect is growth inhibition [40]. Compared to the control group, drought-stressed *I. indigotica* leaves exhibited reduced size, thickness loss, excessive softening, and pronounced wrinkling (Fig. 1A). Under the salt stress, elevated salinity levels progressively suppressed leaf development, resulting in gradual chlorosis, marginal curling, wilting, and sporadic necrotic lesion formation (Fig. 1B). These phenotypic differences suggest that abiotic stresses prevent the accumulation of biomass in *I. indigotica* leaves, compromising their medicinal applicability. Furthermore, stress-induced leaf curling and chlorosis indicate severe cell damage, which may

Table 2 Primer information for qPCR

ID	Gene Symbol		Primer Sequence (5′→3′)	Amplicon Size (bp)	Purification Method
1	*RIBA2*	F	GTCTCAGCTCGTGATAGGGC	20	PAGE
2		R	GCTTCTGTATGCCCTGCTCT	20	PAGE
3	*PsbB*	F	TCTAGTTGCTGGTTGGGCTG	20	PAGE
4		R	TTGGATCAAGAACGGGGTCG	20	PAGE
5	*HSP70*	F	TCACTCCTCTGTCCTTGGGT	20	PAGE
6		R	TCCTTTGTTCGTGCCCTCTC	20	PAGE
7	*PsbQ1*	F	CGATCAAAGTTGGCCCTCCT	20	PAGE
8		R	TGGTGGCAATGGCTGTAAGT	20	PAGE
9	*HSP90*	F	ATTGTGGACTCTCCCTGCTG	20	PAGE
10		R	TATCTCTCAACGCCTGTGCC	20	PAGE
11	*HSP21*	F	AAGTCCGCTACACCGTTCTC	20	PAGE
12		R	TCTCTCTGGTCTTGAGCCCT	20	PAGE
13	*ILVH1*	F	AAGGAAACATCAGCAGGGGG	20	PAGE
14		R	GTGAGAAGTCCCCAGTGAGC	20	PAGE
15	*RBS2*	F	TGCAAGCAACGGAGGAAGAG	20	PAGE
16		R	CACGGTACACAAATCCATGTCG	22	PAGE
17	*STR1*	F	TCGTGTGGGACTGGTGTAAC	20	PAGE
18		R	TAGATCGGCACGTCGGTTTT	20	PAGE
19	*GAPDH*	F	TCTCTGCTCCTCCCTGTTCT	20	PAGE
20		R	ATCCGTTCACACCGACCTTC	20	PAGE

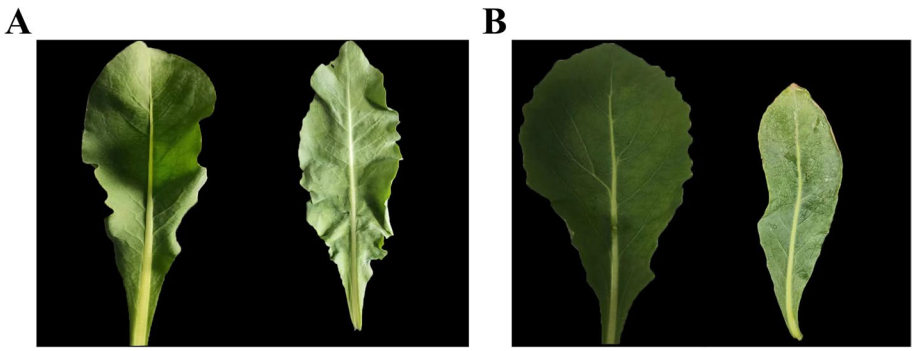

Fig. 1 Phenotypic characteristics of *I. indigotica* leaves under different stress groups. **A** Drought stress. **B** Salt stress

disrupt the biosynthesis of pharmacologically critical secondary metabolites such as indigo and indirubin.

Physiological responses of *I. indigotica* leaves to abiotic stresses

In addition to phenotypic differences, the physiological status of plant leaves is also significantly altered under adverse stress, in particular photosynthetic pigment levels and cell membrane damage. There were significant differences in the levels of photosynthetic pigments of *I. indigotica* leaves. Salt and drought stresses reduced the chlorophyll content by about 34.4%, the carotenoid content by 24%−32%, and the total photosynthetic pigment content by 32.11%−33.5% (Fig. 2A, B). The decrease in photosynthetic pigment content implies an inhibition of photosynthesis, and this inhibition may lead to an insufficient supply of energy required for the synthesis of secondary metabolites, which is detrimental to the accumulation of bioactive constituents. The conjecture that phenotypic changes imply cellular damage caused by adverse stresses was also validated by the results of the REC assay, as there were significant differences in the REC between the stress and control groups (Fig. 2C, D). The t-test results revealed that the RECs of the drought and the high salinity group were significantly greater than those of the control group. This demonstrates that under adverse stresses, the structure and function of the cell membrane of *I. indigotica* leaves are severely impaired, resulting in massive extravasation of intracellular substances. This alteration inhibits normal cellular metabolic activity, thereby limiting the synthesis and accumulation of secondary metabolites.

Levels of bioactive constituents in *Isatidis Folium*

The levels of the bioactive constituents in *Isatidis Folium* were determined by UPLC. Five peaks were identified by comparing the retention times of the samples (Fig. 3B) with those of the standards (Fig. 3A), including 4-hydroxyquinazoline, syringic acid, tryptanthrin, indigo, and indirubin. The RSD of the precision, stability, and repeatability tests ranged from 0.99% to 2.59%, 1.395 to 2.085%, and 0.976% to 3.246%, respectively. The average recoveries ranged from 99.29% to 100.66%, with RSDs ranging from 1.72% to 4.32%. These results demonstrate the good performance and data reliability of the UPLC method. Figure 4 shows the differences in the levels of the five bioactive constituents under different stress conditions. Compared to the control group, the levels of all five constituents were significantly lower in the drought stress group, and except for 4-hydroxyquinazoline, the levels of the other four constituents were also considerably lower in the salt stress group. According to the 2020 edition of the Chinese Pharmacopoeia, the standard level of indirubin is 0.02% as the quality indicator. In this study, the level of indirubin was 0.1% in the control group, 0.046% in the drought group, and 0.018% in the 180 mmol/L salt stress group. Combining the levels of these bioactive constituents and the pharmacopeia standard, it can be concluded that the quality of *Isatidis Folium* was significantly decreased under these two adverse stress conditions.

Transcriptomic and proteomic analyses of *I. indigotica* leaves

Expression levels in transcriptome and proteome

Transcriptomic analysis can be used to compare the number and expression patterns of differentially expressed genes (DEGs) in *I. indigotica* leaves under different stress conditions. A reference-free transcriptome sequencing approach was used, and three RNA treatment groups (control, drought, and salt groups) were sequenced in triplicate. Approximately 510,292,270 raw sequencing reads were generated, and after filtering for low-quality reads, 500,363,048 clean reads were obtained. The raw sequence data reported in this paper have been deposited in the Genome Sequence Archive (Genomics, Proteomics & Bioinformatics 2021) at the

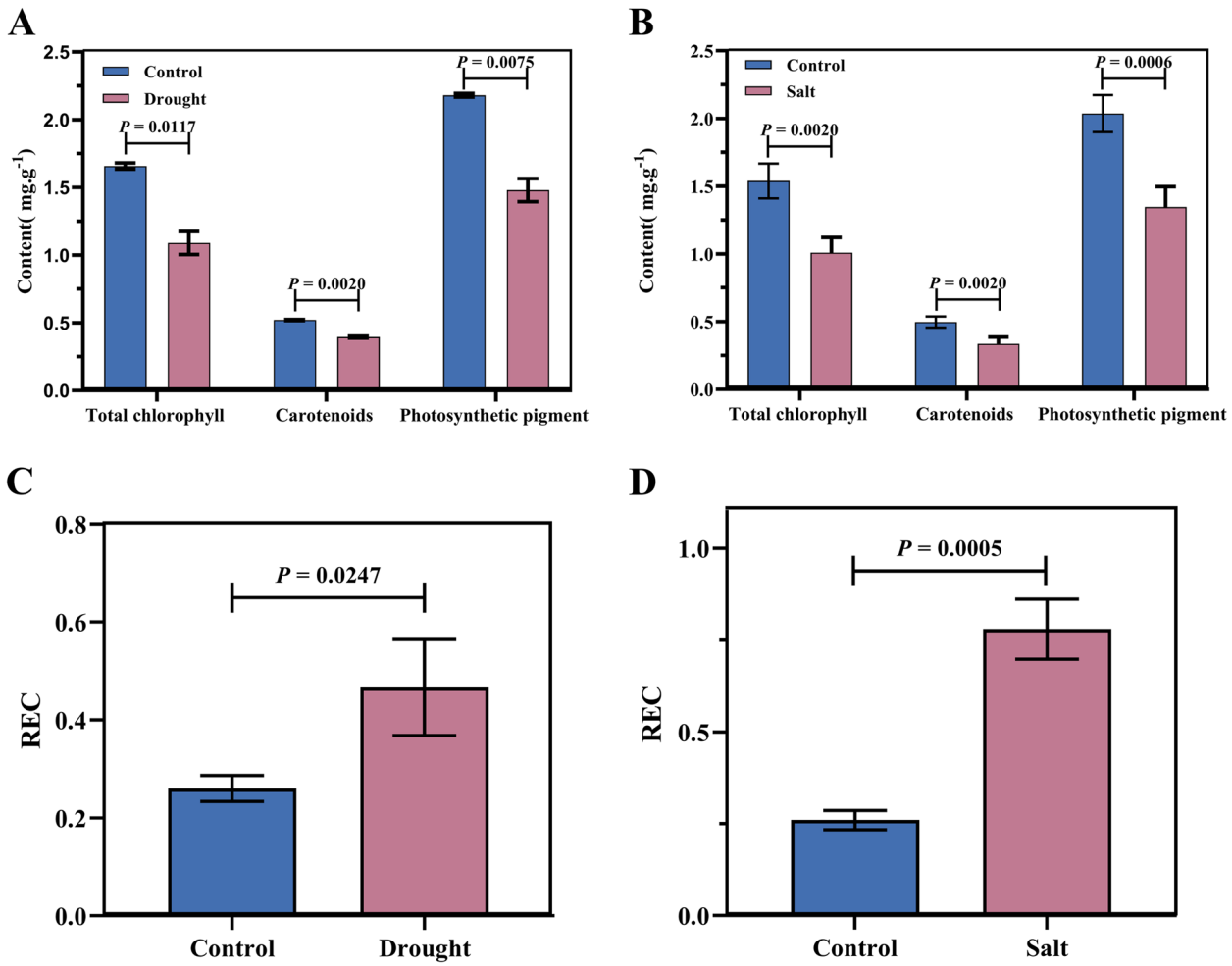

Fig. 2 Physiological characteristics of *I. indigotica* leaves under different stress groups. **A**, **B** The photosynthetic pigment content under drought and salt stress groups. **C**, **D** The REC under drought and salt stress groups

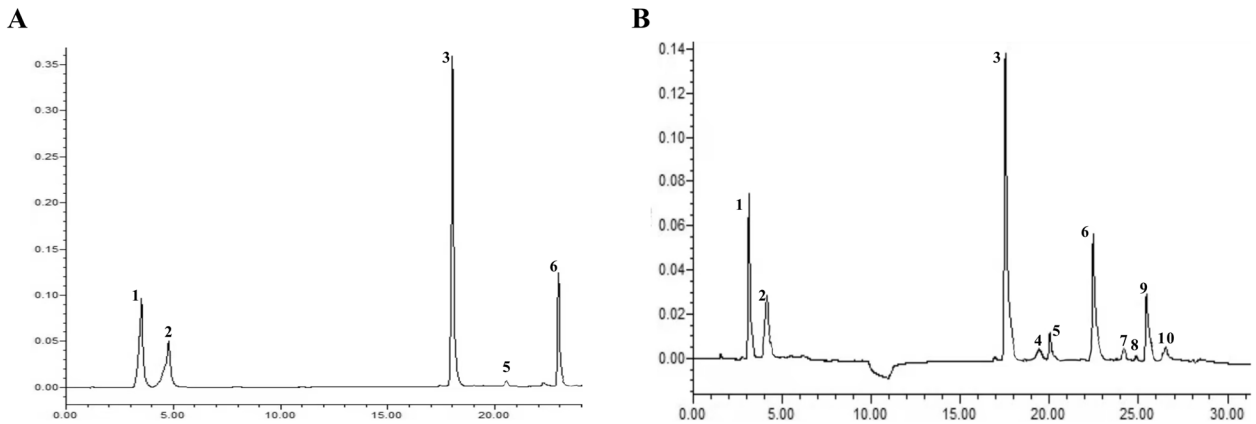

Fig. 3 Representative UPLC chromatograms of the standards (**A**) and samples (**B**). 1, 4-Hydroxyquinazoline; 2, Syringic acid; 3, Tryptanthrine; 5, Indigo; 6, Indirubin. However, the chemical structures of the remaining compounds (4, 7, 8, 9, and 10) are unknown

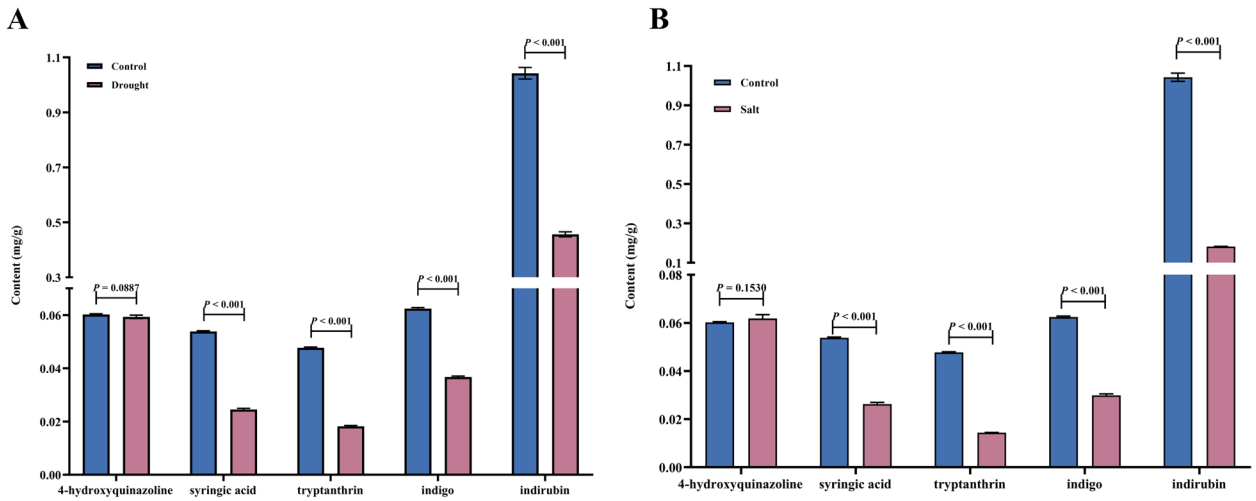

Fig. 4 The t-test analysis results of the bioactive constituents content in *Isatidis Folium* under different stress groups. **A** Drought stress. **B** Salt stress

National Genomics Data Center (Nucleic Acids Res 2022), part of the China National Center for Bioinformation / Beijing Institute of Genomics, Chinese Academy of Sciences (GSA: CRA020651). These data are publicly accessible at https://ngdc.cncb.ac.cn/gsa [44, 45]. The sequencing results revealed that the mean values of Q20 and Q30 for the nine samples were 97.46% and 95.37%, respectively. These results, presented in Table 3, illustrate the high quality of the sequencing data. In the differential expression analysis, genes with a log2-fold change (log2FC) greater than 1 and a *P* value less than 0.05 were identified as DEGs. Compared to the control group, a total of 4,603 DEGs were identified under the drought group, of which 2,414 were significantly up-regulated and 2,189 were significantly down-regulated. In the salt stress group, a total of 6,903 DEGs were enriched, of which 3,377 were significantly up-regulated and 3,526 were significantly down-regulated. The volcano plot (Fig. 5A, B) illustrates the extent of variation in these DEGs, with red and green dots representing up-regulated and down-regulated genes, respectively.

The mass spectrometry proteomics data have been deposited in the ProteomeXchange Consortium (https://proteomecentral.proteomexchange.org) through the iProX partner repository [46, 47] under the accession number PXD058215. The TMT quantitative proteomic experiment yielded a total of 456,486 spectra, 89,514 peptide spectrum matches (PSMs), 29,345 unique peptides, and 4 901 proteins across all stress groups, with 4 897 proteins successfully quantified. Principal component analysis (PCA) was performed on the protein expression profiles of samples subjected to salt and drought stresses. The results indicated that the protein expression of *I. indigotica* leaves under stress conditions differed from that of the control group (Fig. 5E, F). A t-test combined with fold change (FC) was used to analyze the significant differences in protein expression between different groups. Proteins with a *p*-value of less than 0.05 and an FC greater than 1.5 or less than 1/1.5 were considered

Table 3 Quality assessment of the RNA sequencing data

Sample	Raw Data	Clean Reads	Clean Reads (%)	N (%)	Q20	Q30
Control1	49498220	48535196	98.05	0.002648	97.54	95.53
Control2	51737302	50741382	98.08	0.002658	97.52	95.48
Control3	49576802	48615012	98.06	0.002772	97.22	94.91
Drought1	66516698	65207958	98.03	0.002693	97.48	95.42
Drought2	61105506	59865064	97.97	0.002656	97.47	95.41
Drought3	65163286	63846136	97.98	0.002677	97.48	95.42
Salt1	52819148	51801226	98.07	0.006757	97.33	95.11
Salt2	61640216	60486312	98.13	0.002673	97.55	95.57
Salt3	63235092	62047058	98.12	0.002625	97.54	95.51

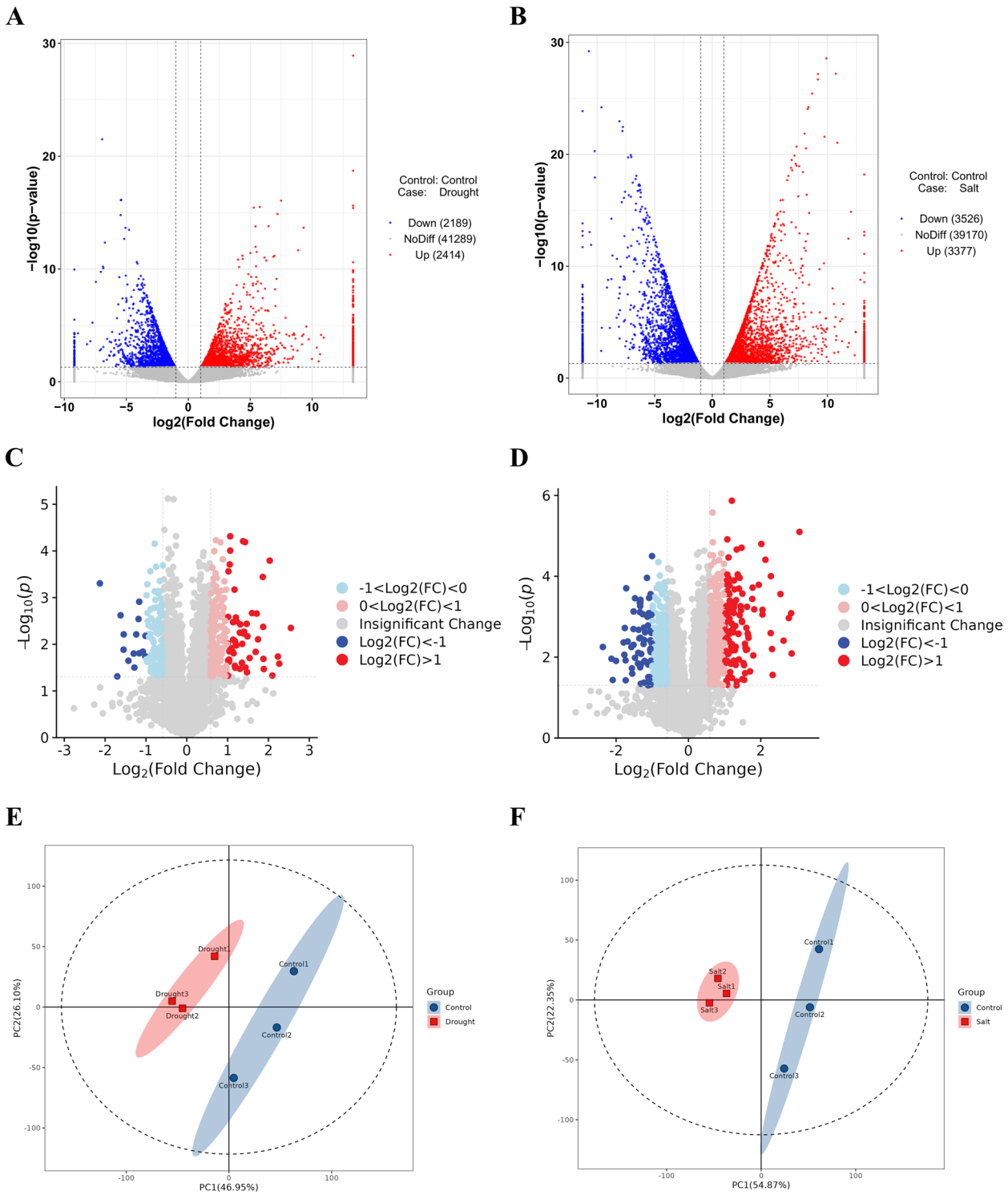

Fig. 5 Volcanic plots and principal component analysis (PCA) of DEGs and DEPs. **A**, **B** The volcano plots of DEGs between the stress and control groups: A, Drought stress; B, Salt stress. **C**, **D** The volcano plots of DEPs between the stress and control groups: C, Drought stress; D, Salt stress. **E**, **F** The score plots of PCA of proteins between the stress and control groups: E, Drought stress; F, Salt stress. The circles and squares represent the sample distributions in the PCA. Control1, Control2, and Control3 represent the three replicates in the control group. Drought1, Drought2, Drought3, Salt1, Salt2, and Salt3 represent the three replicates under drought and salt stress

as differentially expressed proteins (DEPs). Comparative analysis identified 336 DEPs under drought stress (190 up-regulated, 138 down-regulated) relative to controls. Similarly, salt stress induced 761 DEPs (418 up-regulated, 332 down-regulated). The volcano plot (Fig. 5C, D) represents the data as a series of points, where each point corresponds to a protein. The red dots represent significantly up-regulated proteins; the darker the color is, the greater the degree of up-regulation. The blue dots represent significantly down-regulated proteins, with darker colors indicating greater fold downregulation. The gray dots represent undifferentiated proteins.

GO and KEGG enrichment analyses of DEGs

Gene functional enrichment analysis of DEGs was performed using GO and KEGG analyses. In the "Drought vs. Control" analysis, a total of 4689 biological processes (BP), 657 cellular components (CC), and 1520 molecular functions (MF) were identified. Figure 6A shows node information with high significance. For MF, the significantly enriched GO terms included phospholipase activity, transmembrane transporter activity, and carbohydrate binding. The main enriched CCs among the DEGs were associated with membranes, photosystem I reaction centers, and quasi-cysts. In the BP category, the majority of DEGs were significantly enriched in processes related to photosynthesis, stimulus responses, and responses to abiotic stimuli. A total of 1,324 DEGs were mapped to 123 KEGG pathways. Among the top twenty pathways, 297 DEGs were enriched in metabolic pathways, with 115 genes showing significant up-regulation and 182 genes showing significant down-regulation. The most important pathways were those related to photosynthesis, phytohormone signaling, and carotenoid biosynthesis (Fig. 6B).

In the "Salt vs. Control" analysis, most DEGs were enriched in response to external stimuli, with notable enrichment in response to heat. Figure 7A shows the GO enrichment results. In the CC category, the most significant enrichment was observed in entries related to the cellular septum. In the MF category, the most significant functional categories were transporter activity and flavin adenine dinucleotide incorporation. In the BP category, the majority of DEGs were significantly enriched in processes related to response to hormone and oxygen-containing compounds and the polysaccharide catabolic process. A total of 1,913 DEGs were mapped to 129 KEGG pathways, 363 of which were enriched in metabolic pathways, with 202 genes showing up-regulation and 161 genes showing down-regulation. The most prominent pathways were those related to plant hormone signaling, photosynthesis, and indole alkaloid biosynthesis (Fig. 7B). Among the DEGs, those involved in photosynthesis were significantly down-regulated in both the drought and salt stress groups, with 22 and 21 DEGs down-regulated, respectively, accounting for 99% of the total DEGs in this pathway. The indole alkaloid biosynthesis pathway was significantly down-regulated under salt stress conditions. The plant hormone signaling

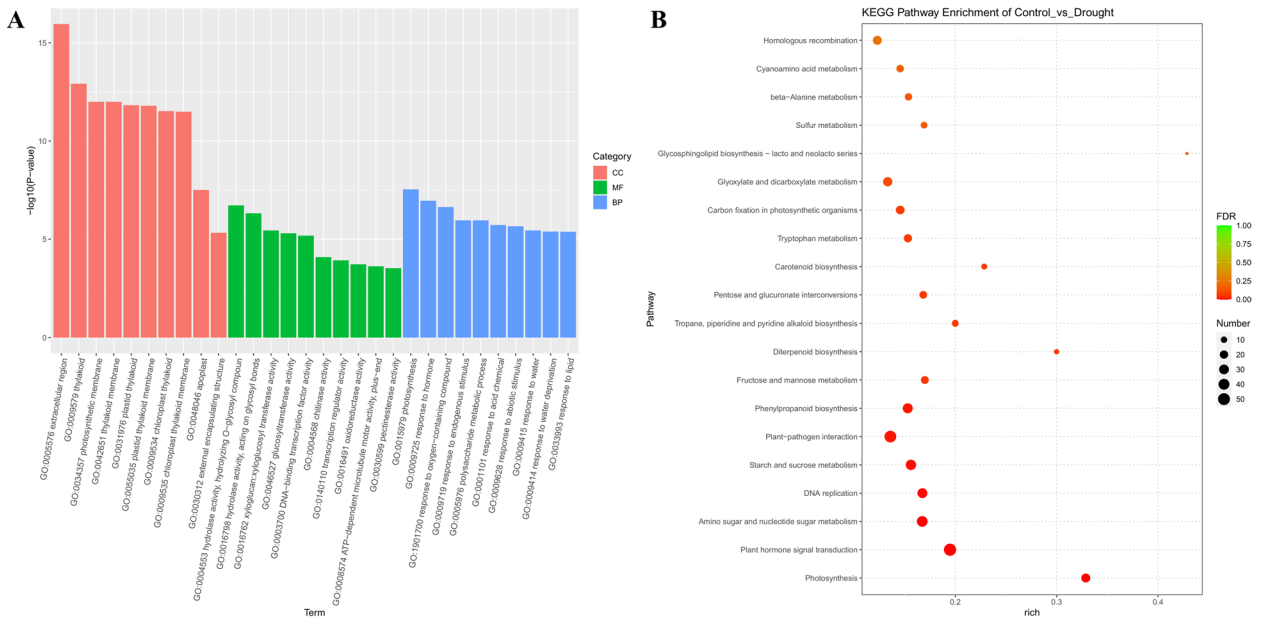

Fig. 6 GO and KEGG enrichment analyses of DEGs in the "Drought vs. Control" group. **A** GO enrichment analysis. **B** KEGG enrichment analysis

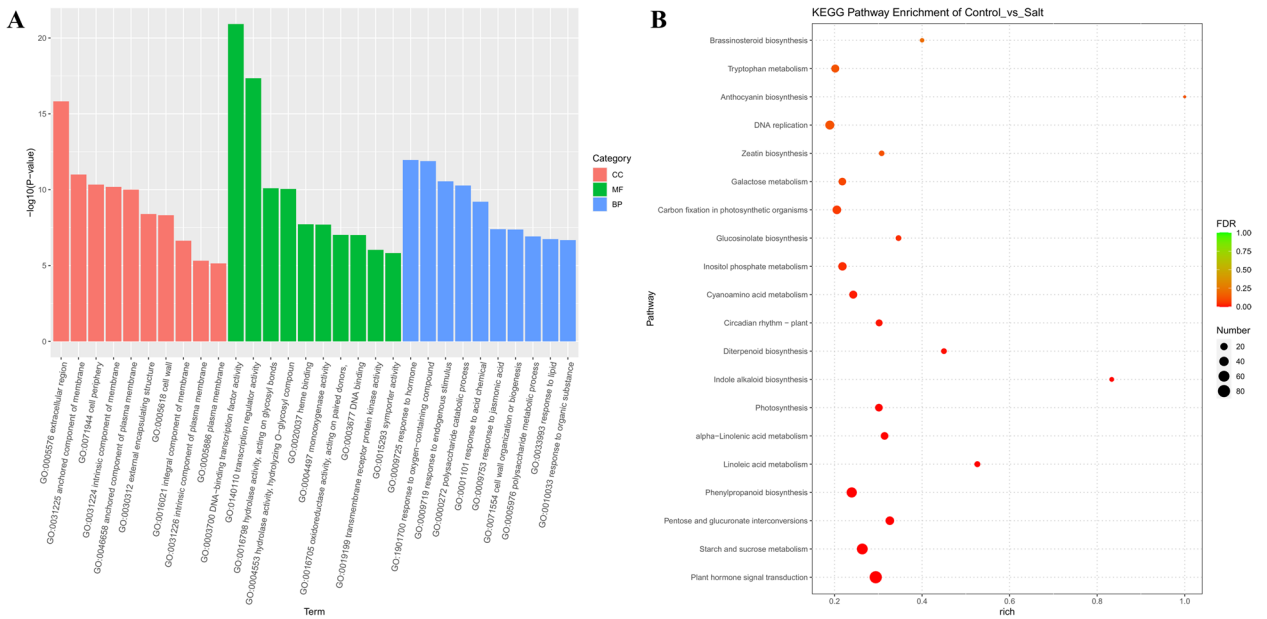

Fig. 7 GO and KEGG enrichment analyses of DEGs in the "Salt vs. Control" group. **A** GO enrichment analysis. **B** KEGG enrichment analysis

pathway was enriched with a large number of up-regulated genes under both stress conditions.

GO and KEGG enrichment analyses of DEPs

A comprehensive analysis of the biological functions of DEPs can be performed using GO annotations. In the "Drought vs. Control" analysis, a total of 94 GO terms were obtained, including 62 BP terms, 4 CC terms, and 28 MF terms. DEPs were enriched primarily in sulfur compound metabolic, biosynthesis of sulfur-containing amino acids, photosynthesis, photosystem, transferase activity, and methionine adenosyl transferase activity (Fig. 8A). To gain further insight into the biological functions of the yet undiscovered DEPs, a KEGG enrichment analysis was performed. The results revealed that the DEPs were enriched in 38 signaling pathways, predominantly photosynthesis-related pathways, amino acid synthesis, ribosome, biosynthesis of secondary metabolites, and porphyrin metabolism (Fig. 8B).

A total of 89 GO terms, including 48 BP terms, 9 CC terms, and 32 MF terms, were identified in the "Salt vs. Control" analysis. The DEPs annotated by GO were

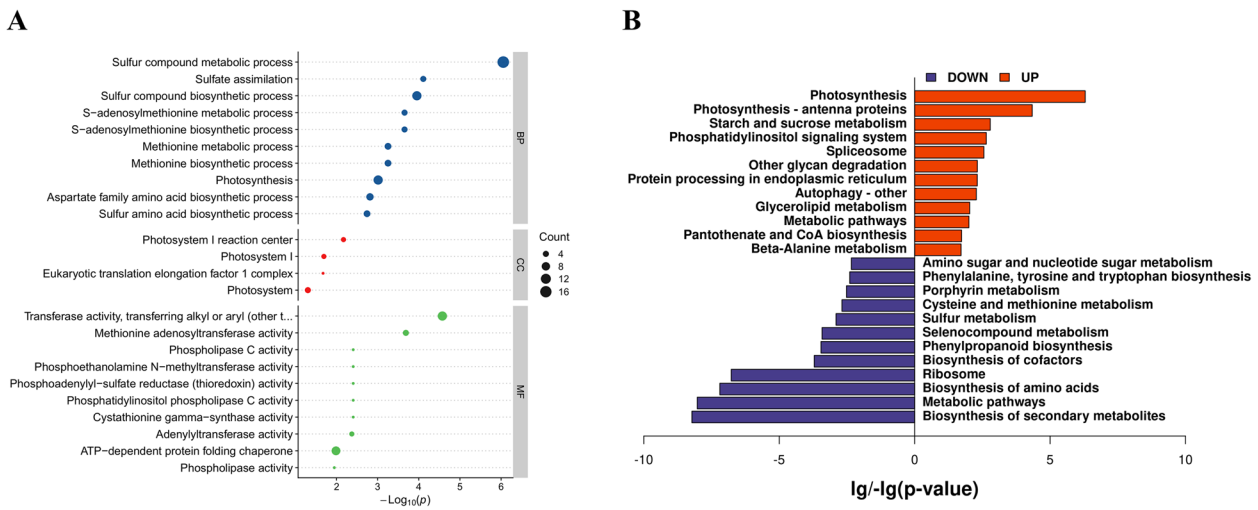

Fig. 8 GO and KEGG enrichment analyses of DEPs in the "Drought vs. Control" group. **A** GO enrichment analysis. **B** KEGG enrichment analysis

predominantly enriched in the sulfur compounds metabolism, transmembrane transport, membranes, microtubules, oxidoreductase activity, and methionine adenosyltransferase activity (Fig. 9A). In the KEGG analysis, the DEPs enriched in 44 signaling pathways, including 35 metabolism-related pathways, 2 cellular process-related pathways, 2 environmental information processing-related pathways, 3 genetic information processing pathways, and 1 biosystem-related pathway. The DEPs were enriched primarily in pathways related to secondary metabolite biosynthesis, ribosomes, amino acid metabolism, carbon metabolic-related processes, and photosynthesis (Fig. 9B).

Joint analysis of transcriptome and proteome

Expression levels of corresponding DEGs and DEPs (cor-DEGs-DEPs)

By identifying DEGs and DEPs in *I. indigotica* leaves subjected to salt and drought stress, we aimed to gain insight into the regulatory mechanisms governing the impact of these stresses on the quality of *Isatidis Folium* at the gene and protein levels. To ensure the reliability of the data, we performed an integrated proteomic–transcriptomic analysis using a combined approach to analyze the DEPs and DEGs, as illustrated in Fig. 10. Compared with those in the control group, 4,603 DEGs and 336 DEPs were enriched in the drought stress group, of which 95 cor-DEG-DEPs were matched. Among these matched proteins, a total of 69 presented the same expression trend, including 46 up-regulated and 25 down-regulated proteins. The majority of the up-regulated proteins were related to heat shock, whereas the majority of the down-regulated proteins were related to chlorophyll synthesis and photosynthesis. In the salt stress and control groups, there were 6903 DEGs and 761 DEPs, with 298 matched cor-DEGs-DEPs. Among these matched proteins, 245 exhibited the same expression trend, including 142 up-regulated and 103 down-regulated proteins. Most of the up-regulated proteins were heat shock proteins, ABC transporters, and peroxisome-related proteins. The majority of the down-regulated proteins were associated with chloroplasts and photosynthesis.

KEGG pathway enrichment analysis of cor-DEGs-DEPs

A combined biomics KEGG pathway enrichment analysis was then performed to identify the biological pathways in which the cor-DEGs-DEPs were primarily involved. The results revealed that DEPs and DEGs exhibited comparable expression levels of primary metabolites, including several amino acids. Furthermore, an increase in these amino acids was identified as a key indicator of improved plant resistance. In the case of the phytohormone and photosynthesis systems, the number of DEPs was significantly lower than that of DEGs. Additionally, in the photosynthesis system, the expression trends of genes and proteins were reversed, indicating the presence of intermediate regulatory mechanisms between genes and proteins during the metabolism of more complex pathways. These findings suggest that the expression patterns of these two factors may not be directly parallel. Concerning porphyrin metabolism, tryptophan metabolism, indole alkaloid biosynthesis, and the biosynthesis of other secondary metabolites, the trends in gene and protein expression were largely consistent, with the majority showing down-regulation (Fig. 11).

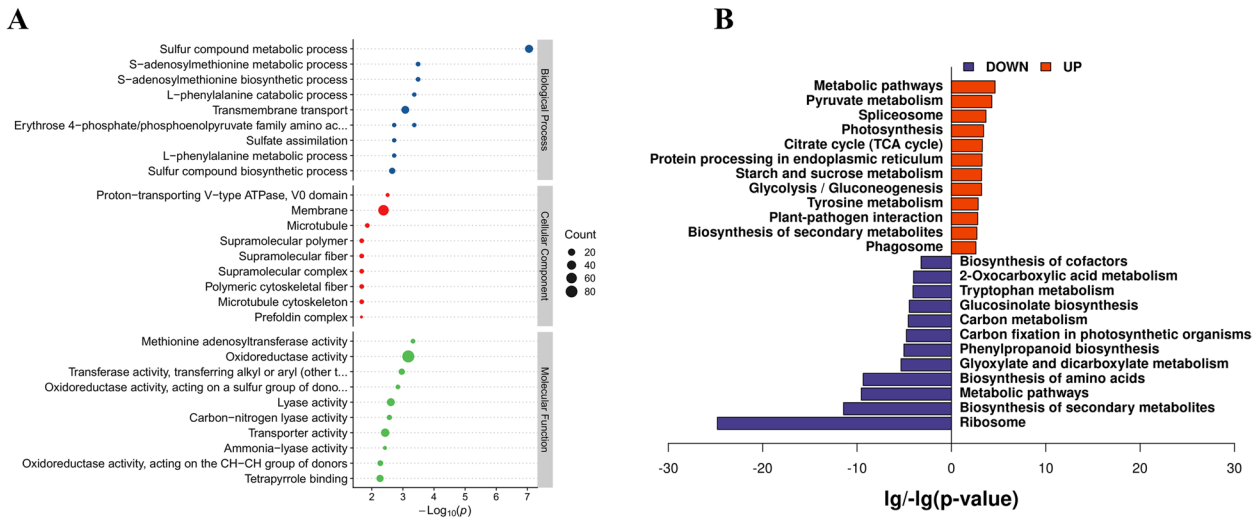

Fig. 9 GO and KEGG enrichment analyses of DEPs in the "Salt vs. Control" group. **A** GO enrichment analysis. **B** KEGG enrichment analysis

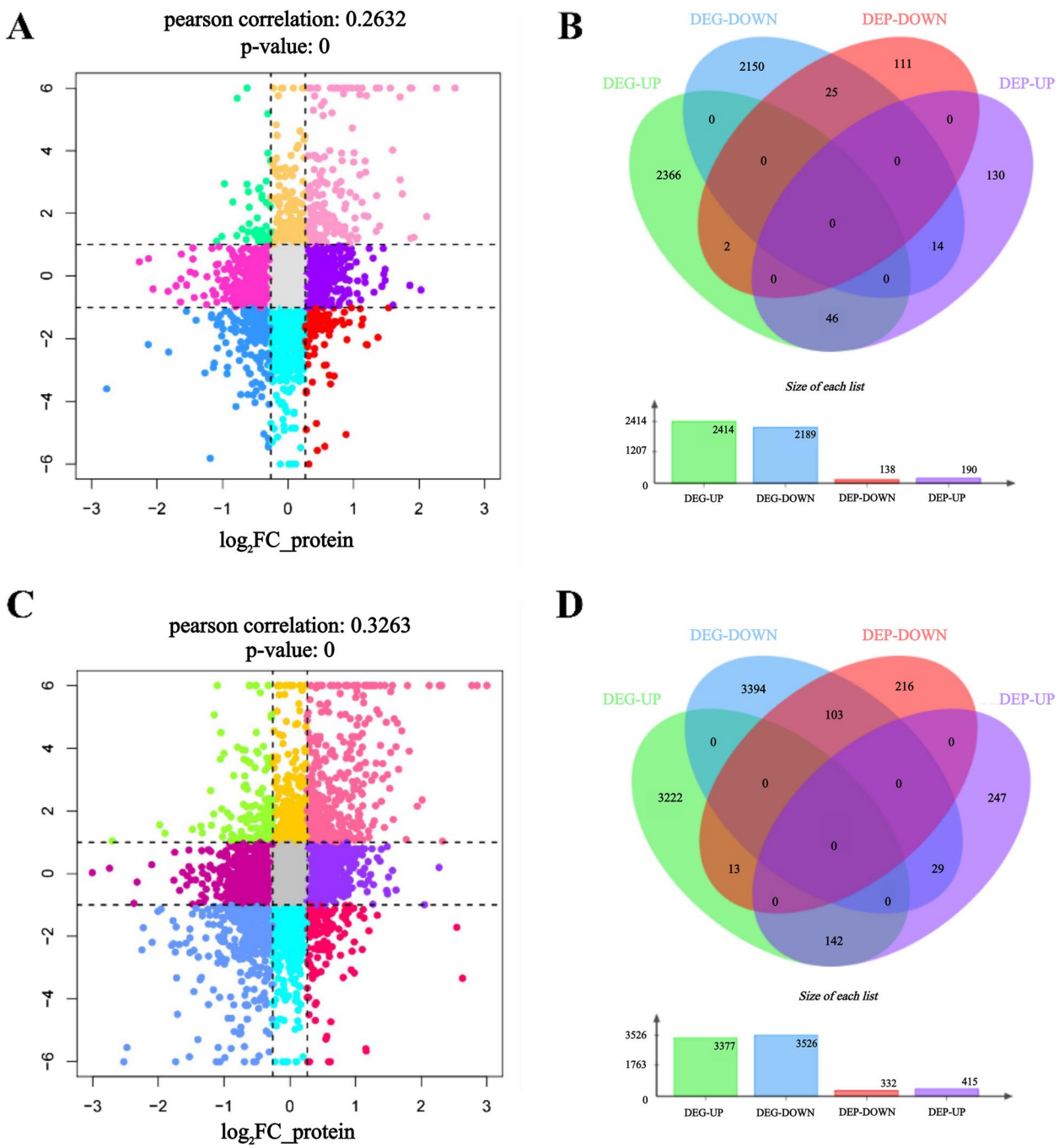

Fig. 10 Nine quadrant and Venn diagrams of the results of the transcriptomic–proteomic correlation analysis. **A**, **C** Nine-quadrant plots of the drought and salt stress groups compared with the control group. Scatterplot of expression correlations for all quantified proteins and their associated genes. The x-axis represents the log2 ratio of the protein, and the y-axis represents the log2 ratio of the transcript; black dotted lines represent the different thresholds; each dot represents a gene or protein; gray dots represent unchanged genes or proteins. It is divided into nine quadrants from left to right and from top to bottom with black dotted lines. **B**, **D** Venn diagrams of the transcriptomic-proteomic correlation analysis of the quantitative and differential expression levels of the drought and salt stress groups, respectively

qPCR validation

To further validate the results of the omics data, 9 significant DEGs were selected for qPCR analysis. Figure 12 shows the expression levels of key regulators that may be associated with the differences in *I. indigotica* leaves under different stress conditions. The trends in the expression of the unigenes from the qPCR and RNA sequencing analyses were largely consistent. The results

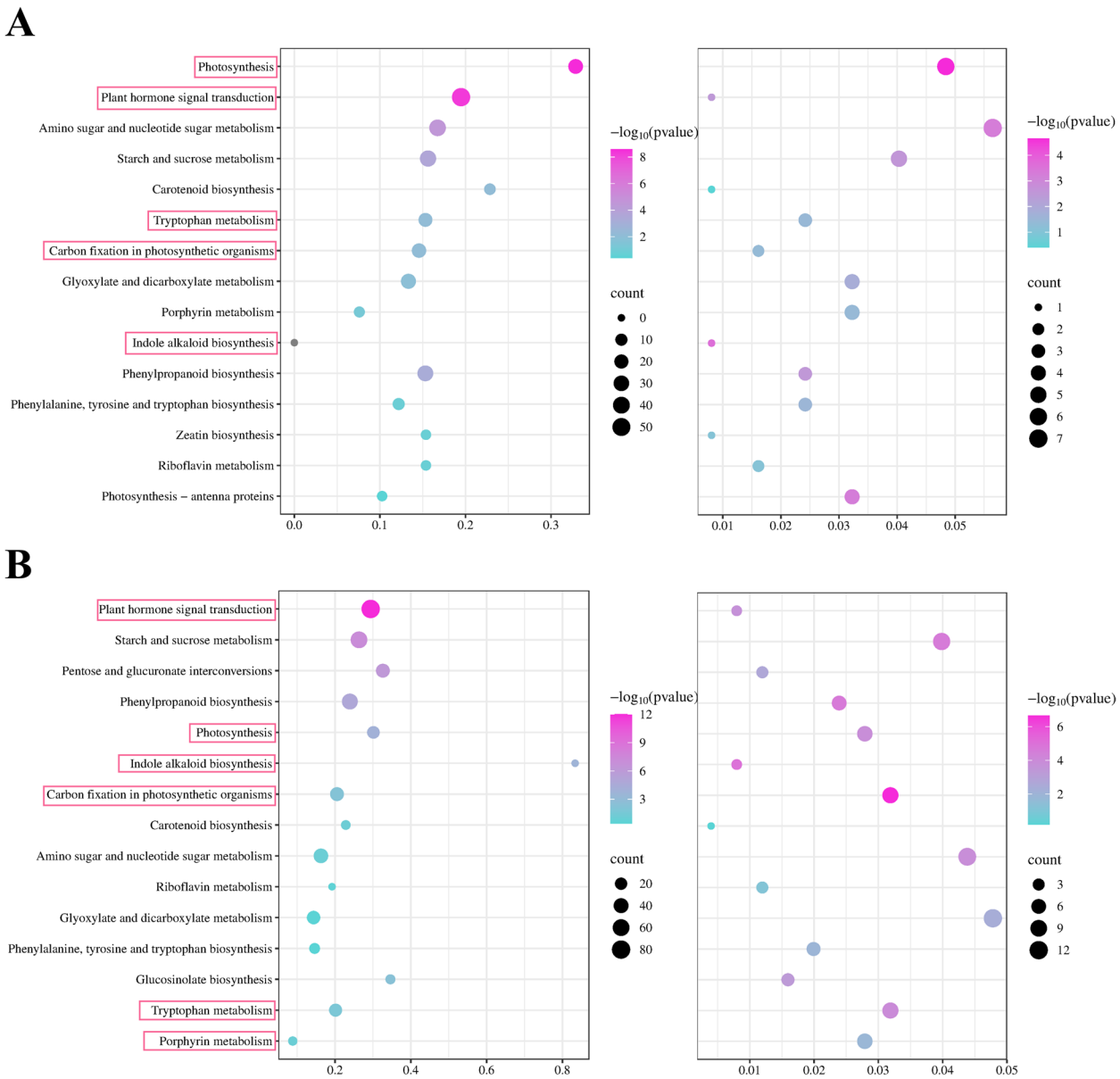

Fig. 11 KEGG annotation and enrichment of 15 pathways of cor-DEGs-DEPs for association analysis. **A** Drought stress. **B** Salt stress. The left side represents the KEGG enrichment bubble plot of the DEGs, and the right side represents the KEGG enrichment bubble plot of the DEPs. The vertical coordinate represents the pathway term, the horizontal axis represents the enrichment rate, and the size of the bubbles is proportional to the number of proteins or genes enriched in that pathway. The different colors of the bubbles represent different *P* values

confirm the accuracy and reliability of the omics data, demonstrating that the sequencing data can accurately reflect the effects of abiotic stressess on *I. indigotica*.

Discussions

Mechanisms by which drought and salt stresses affect the growth and physiological status of *I. indigotica*

Salt stress and drought stress represent two predominant abiotic stressors in plant systems. These stresses promote the excessive accumulation of ROS, leading to oxidative stress damage in tissue cells. This disruption affects the selective permeability of the cell membrane [48], resulting in the extravasation of intracellular substances, as confirmed by the significant increase in the REC observed under stress conditions in this study. Concomitantly, pronounced degradation of photosynthetic pigments occurs [48, 49], impairing key physiological processes and ultimately compromising plant stress tolerance. Photosynthetic machinery is particularly vulnerable to abiotic stress perturbation. The process of photosynthesis is particularly

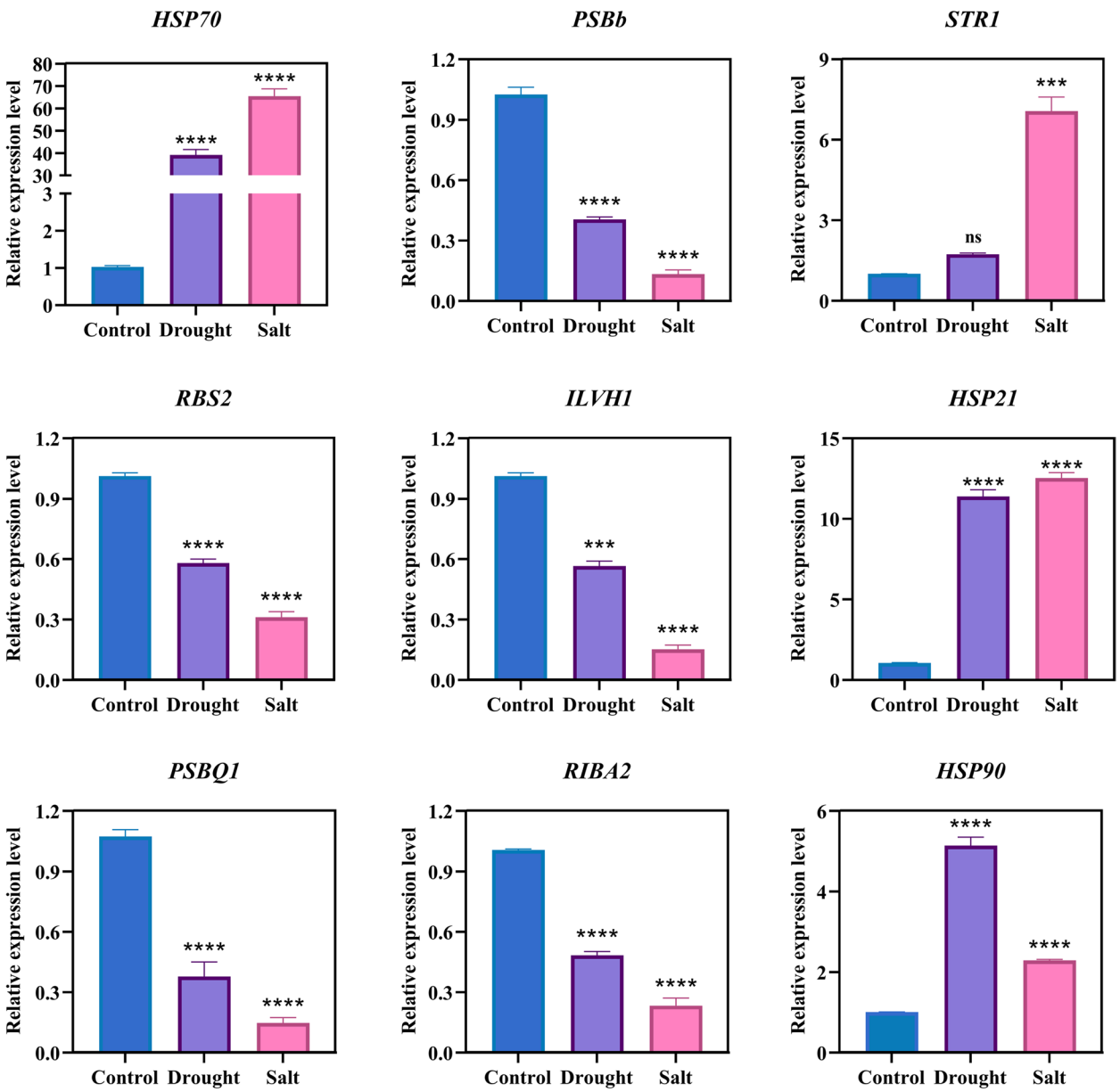

Fig. 12 qPCR analysis of selected DEGs. ns > 0.05; *$P \leq 0.05$; **$P \leq 0.01$; ***$P \leq 0.001$; ****$P \leq 0.0001$

affected when green plants are subjected to abiotic stresses. The reasons for this outcome may include a reduction in the concentration of photosynthetic pigments, particularly chlorophyll, damage to the photosystems, and impaired carbon fixation. The results of the present study revealed that the content of photosynthetic pigments significantly decreased in large green leaves under stress.

Porphyrin metabolism pathway-mediated reduction of photosynthetic pigment levels

The porphyrin metabolism is a key biochemical pathway involved in the synthesis and degradation of porphyrins, as well as the biological pathway for the synthesis and degradation of many important pigments, including photosynthetic pigments, in green plants. Therefore, it plays an important role in maintaining the homeostasis of photosynthetic pigments. Transcriptome analysis revealed that, in the salt stress group, three genes were up-regulated, four genes were down-regulated, two proteins were up-regulated, and five proteins were down-regulated. In contrast, the drought stress group exhibited six DEGs and four DEPs, all of which were significantly down-regulated. Among the genes and proteins that were upregulated in the salt stress group, *RCCR* played a

significant role. *RCCR* catalyzes pivotal reactions in chlorophyll catabolism [50]. Consequently, the up-regulation of *RCCR* expression suggests an increase in chlorophyll degradation. Among the down-regulated genes and proteins, *POR* and *HemB* had more significant biological functions. *POR* catalyzes the phototransformation of protochlorophyllide to chlorophyllide and is a key regulatory factor in the chlorophyll synthesis process [51]. The expression of the Hem protein family, particularly *HemB*, has a positive regulatory effect on chlorophyll biosynthesis [52, 53]. Therefore, the down-regulation of *POR* and *HemB* expression, which blocks chlorophyll synthesis, maybe another important mechanism contributing to the reduction in photosynthetic pigments, especially chlorophyll content, under stress conditions in *Isatidis Folium*.

Damage to the photosynthetic system and photosynthesis

The transcriptomic analysis demonstrated that a considerable number of genes were markedly enriched for photosynthesis in response to stress conditions. Specifically, 22 DEGs were identified, 21 of which were significantly down-regulated in the salt stress group. In the drought stress group, 24 DEGs were identified, 22 of which were significantly down-regulated. Moreover, a significant reduction in the expression levels was observed for the majority of proteins within the *Psa* and *Psb* families, which serve as essential components of photosystem I (PSI) and photosystem II (PSII), respectively [54]. PSII, located in the thylakoid membrane, oxidizes water by absorbing light energy to release oxygen molecules and generate electrons. The electrons are transferred to PSI via plastoquinone, the Cyt b6/f complex, and plastocyanin and are then reduced from NADP to NADPH by ferritin transfer [55, 56]. In this process, *PsbB* and *PsbQ1* play significant roles. *PsbB* encodes the CP47 protein, which is a component of the PSII core complex. It binds chlorophyll and catalyzes primary light-induced photochemical processes [57]. *PsbQ1*, encoding photosystem II oxygen-evolving enhancer protein 3-1, is involved in the formation of the oxygen-evolving complex of PSII, which catalyzes the oxidation of water molecules and the release of oxygen and electrons [58, 59]. Omics analysis showed that the relative expression levels of *PsbB* and *PsbQ1* were significantly down-regulated under both stress conditions, indicating that these stresses have significant negative effects on the structure and function of PSII, leading to photosystem damage and severe inhibition of photosynthesis. The proteomic analysis revealed that DEPs were enriched predominantly in the photosynthesis pathway under both stresses, with seven and five DEPs, respectively, but were significantly up-regulated, in contrast to the transcriptomic results. There are complex feedback regulatory mechanisms in the photosynthetic system. When the photosystem is impaired, plants may increase the levels of key proteins through other pathways to ensure that photosynthesis proceeds as normally as possible or improve the homeostasis and survival time of these proteins.

RBS2 and RIBA2-mediated the inhibition of carbon fixation process in photosynthesis

Combined omics analysis revealed that the expression of *RBS2* and *RIBA2* was significantly down-regulated under both stress conditions. *RBS2*, also known as *RBCS2*, encodes one of the small subunits of RuBisCO, a key enzyme affecting the rate of photosynthesis that catalyzes the binding of ribulose-1,5-bisphosphate and carbon dioxide to form two molecules of glycerol-3-phosphate. This process is the first step of carbon fixation in photosynthesis [60, 61]. Although the small subunit is not catalytic, it is essential for RuBisCO activity. *RBS2* is therefore essential for carbon fixation and photosynthesis. Moreover, *RBS2* is involved in plant stress tolerance, and its increased activity helps plants resist various external environmental stresses [62]. Riboflavin biosynthesis protein 2, encoded by *RIBA2*, is a key protein in the process of riboflavin (also known as vitamin B2) biosynthesis. Riboflavin functions in the cell mainly as flavin coenzymes (FAD and FMN) and is involved in numerous biological processes, such as plant defense responses, cellular redox homeostasis, chloroplast pigment synthesis, photosynthesis and respiration, and the synthesis of natural secondary metabolites [63]. In the photoreaction, FAD acts as a cofactor for ferritin NADP reductase (FNR). In PSI, FNR accepts electrons from ferritin and transfers them to $NADP^+$, reducing $NADP^+$ to NADPH for carbon fixation [64, 65]. Thus, *RIBA2* also plays a crucial role in carbon fixation in photosynthetic organisms. These findings suggest that the downregulation of *RBS2* and *RIBA2* expression implies that carbon fixation is inhibited under stress conditions, resulting in a decrease in photosynthesis. This also led to a reduction in the plant's stress tolerance and an inability to respond positively and promptly to external environmental stresses. In addition, salt and drought stresses promote excessive accumulation of ROS, causing oxidative stress and leading to oxidative damage to the membrane system. This can damage the structure and function of the thylakoid membrane, affecting the normal function of photosynthetic pigments and electron transport proteins, as well as the activity and stability of photosynthesis-related enzymes.

The role of heat shock protein initiation in the response of *I. indigotica* to adversity

Heat shock proteins, encoded by the *HSP* gene family, are a class of highly conserved proteins that are

activated when plants are exposed to adverse stresses such as high temperature, low temperature, drought, and salinity. They act as molecular chaperones, helping to refold misfolded proteins back to their normal conformation, thereby maintaining cellular homeostasis [66, 67]. Transcriptomic and proteomic analyses revealed that the *HSP* family, e.g. *HSP21*, *HSP22*, and *HSP70*, is abundantly expressed under both salt and drought stress conditions. Both *HSP21* and *HSP22* are members of the small heat shock protein family. Previous studies have shown that small heat shock protein members regulate plant growth and development [68] and play important roles in the response to various abiotic stresses [69, 70]. Under stress conditions, plants can protect the PSII complex by increasing the expression of small heat shock proteins, even if the expression level of related genes decreases [71, 72]. Activated small heat shock proteins act as molecular chaperones that are capable of restoring and maintaining the stable conformation of photosystem proteins in response to the adverse effects of stress-induced gene expression. Thus, although the expression of photosystem genes was down-regulated under stress, the activation of small heat shock proteins prolonged the survival of these proteins, resulting in an increase rather than a decrease in the levels of the detected proteins, which may indicate a compensatory mechanism in response to environmental changes or stresses in *I. indigotica*. In addition, the heat shock 70 kDa protein family, an important member of the heat shock protein family, is widely involved in plant growth and development and plays important regulatory roles in response to adversities such as low temperature, high temperature, drought, and salt stress [73–76]. The overexpression of *HSP70* has been reported to be positively correlated with heat tolerance in plants [77] and to improve salt and drought tolerance in plants [78, 79]. In addition, *HSP70*, in collaboration with other molecular chaperones, is a key factor in facilitating the folding of proteins synthesized from scratch, contributes to the translocation of precursor proteins into organelles, and is responsible for the degradation of damaged proteins under stress conditions [80]. In this study, heat shock proteins, such as *HSP21*, *HSP22*, and *HSP70*, were significantly up-regulated under both salt and drought stress, which is consistent with the findings of previous studies, implying that they play active roles in the response to salt stress and drought stress in *I. indigotica*. Despite the fact that the levels of the relevant proteins were increased against the background of decreasing levels of the relevant genes, the growth and physiological status of *I. indigotica* ultimately deteriorated due to overly intense adverse stresses that exceeded the range of its compensatory capacity.

Identification of the quality of *Isatidis Folium* based on multi-component quantitative analysis and the potential mechanisms of inhibition of bioactive constituents synthesis under adverse stresses

Multi-component content determination based on UPLC revealed that the levels of indigo, indirubin, tryptanthrin, and syringic acid in *Isatidis Folium* were significantly reduced under stress conditions. Indigo and indirubin are bisindole alkaloids, whereas tryptophan is a quinoline indole alkaloid. The synthesis mechanisms of indigo, indirubin, and tryptophan in plants have not yet been fully elucidated. However, their synthesis is related to tryptophan metabolism, and tryptophan and indole are key substances in the synthesis of these three components [81, 82]. In the phenylalanine, tyrosine, and tryptophan synthesis pathway, chorismic acid generates indole and tryptophan in a multistep reaction catalyzed by telomere repeat-binding proteins and tryptophan synthases [83]. In the tryptophan metabolic pathway, tryptophan can be converted to indole, which is then converted to indoxyl (3-hydroxyindole) via a process catalyzed by cytochrome P450 monooxygenase [84]. Indoxyl groups are toxic and chemically active and are converted to chemically stable and nontoxic indican, which is catalyzed by UDP-glucosyltransferase and stored in vesicles. Upon plant damage or even cell death, the vesicle membrane ruptures, and indican is released. Indican is reduced by endogenous β-glucosidase to indoxyl, which is then oxidized and dimerized by oxygen in the air to form indigo [85, 86]. In addition to this pathway, indoles can also be hydroxylated at the 2-position and then oxidized to isatin, which can be stably present for long periods in the leaves of *I. indigotica*; during sun-drying, isatin dimerizes to form indirubin [87, 88] and is also capable of dehydrative condensation with anthranilate to form tryptophan [87, 89]. Transcriptomic and proteomic analyses revealed that the expression of telomere repeat-binding protein 3 (encoded by *TRP3*) was significantly down-regulated under salt stress, and the expression of the tryptophan synthase alpha chain (encoded by *TRPA*) and beta chain (encoded by *TRPB*) was significantly down-regulated under both stresses. These three factors play crucial roles in the synthesis of indole and tryptophan. *TRP3* specifically binds to plant telomeric double-stranded DNA sequences, induces DNA bending, and plays an important role in maintaining telomere structure and protecting chromosome ends [90]. Tryptophan synthase is a heterotetramer with an αββα subunit structure. The α-subunit, which is essential for tryptophan biosynthesis, cleaves 3-indolylglycerophosphate to indole and glyceraldehyde 3-phosphate, contributes to tryptophan-independent indole biosynthesis, and plays an important role in growth hormone synthesis. The β-subunit enzymatically synthesizes

L-tryptophan using indole and L-serine as substrates [91, 92]. Therefore, we believe that adverse stress inhibits indole and tryptophan biosynthesis by down-regulating the expression of *TRP3*, *TRPA*, and *TRPB*, resulting in blockage of the indigo, indirubin, and tryptophan biosynthesis pathways, which leads to a decrease in the accumulation of the bioactive constituents of *Isatidis Folium* and thus affects herbal quality.

In addition, five up-regulated DEGs, one up-regulated DEP, and one down-regulated DEP were enriched in the indole alkaloid synthesis pathway in the salt stress group, and one significantly up-regulated DEP was also identified via proteomic analysis of the drought stress group. Surprisingly, one gene, STR1, was significantly up-regulated in all the tested groups. *STR1* encodes strictosidine synthase, a key enzyme in indole alkaloid biosynthesis, and is also involved in biological processes such as plant stress tolerance and pollen development [93]. Strictosidine synthase is located in the pharyngeal position during indole alkaloid biosynthesis [93] and has a vital regulatory role. Under stress conditions, plants are exposed to negative effects such as oxidative damage and impaired photosynthesis. As a result, the synthesis of secondary metabolites is also diminished. At this time, to cope with the negative effects of stress, *Isatidis Folium* will activate an emergency response mechanism, which may compensate for the reduction in the rate of indole alkaloid synthesis due to the negative effects by up-regulating the expression of *STR1* and related factors, which may constitute another important regulatory mechanism of *Isatidis Folium* in response to the effects of high salt stress and drought stress on its herbal quality. Similarly, given the severe impairment of cellular and metabolic activity and the limited sources of raw materials and energy under the severe stress, despite the up-regulation of the levels of some specific proteins involved in the synthesis of secondary metabolites, this response mechanism was no longer sufficient to compensate for the damage caused by such adverse stresses. This influence ultimately led to the inhibition of the synthesis and accumulation of bioactive components in *I. indigotica* leaves, which implied a reduction in the quality of *Isatidis Folium*.

Limitations and prospects

This study is the first to use the multi-omics technique to investigate the quality formation mechanisms of *Isatidis Folium* under the abiotic stress, which will effectively fill the gap of "adversity-herbal quality-mechanism". Through this study, we have identified the potential pathways through which salt and drought stresses may affect the quality of *Isatidis Folium* in terms of physiological indicators and accumulation of bioactive constituents, and we have preliminarily identified the key proteins and genes. Based on the above analysis, a schematic diagram was constructed to illustrate the potential pathway through which drought and salt stresses affect the quality of *Isatidis Folium* and the response mechanisms of plants to stressful environments (Fig. 13). However, this study is not sufficient to determine the specific value of the quality control index for the time being, just as the Chinese Pharmacopoeia stipulates that the content of indirubin should be not less than 0.020%. Nonetheless, this study can help to develop quality standards and optimize cultivation conditions from the level of bioactive constituents and multi-omics analyses to achieve real quality "control" during the cultivation process of *Isatidis Folium*. Meanwhile, this study can effectively guide the breeding of high-yielding and high-quality *I. indigotica* varieties in the field of molecular breeding. All these measures can help to solve the current dilemma of low-quality and heterogeneous quality control methods of Isatidis Folium, and can also provide a research basis for the quality control system and germplasm resource development of Chinese herbs.

Conclusion

In this study, a UPLC-based multi-component quantitative analysis method was developed and validated for the simultaneous determination of the levels of various bioactive constituents of *Isatidis Folium*, and four constituents, including syringic acid, tryptanthrine, indigo, and indirubin, were established as quality control indicators. Biological pathways such as porphyrin metabolism, photosynthesis, and carbon fixation in photosynthetic organisms were the major causes of photosystem phototoxicity and deterioration of growth status in *I. indigotica* leaves under stress conditions, where *HemB*, *PsbB*, *RBS2*, and *RIBA2* play important roles. Meanwhile, pathways such as phenylalanine, tyrosine, and tryptophan synthesis, tryptophan metabolism, and indole alkaloid synthesis were the major causes of stress reduction of bioactive constituents content, where *TRPA*, *TRPB*, and *TRP3* play important roles. Meanwhile, in the differential expression analysis of the transcriptome as opposed to the proteomic analysis, we also determined the potential pathway of HSP-based expression regulation in response to external stresses. Based on the integration of chemical analysis and multi-omics techniques, we propose a novel hierarchical quality control scenario for *Isatidis Folium*: the quantification of the main chemical indicators was identified based on UPLC to assess the levels of the bioactive components; the genetic indicators associated with the biosynthesis of active components and stress response were monitored using qPCR analysis to assess the excellence of the cultivation conditions and plant adaptation to the environment. This work presents, for the first time,

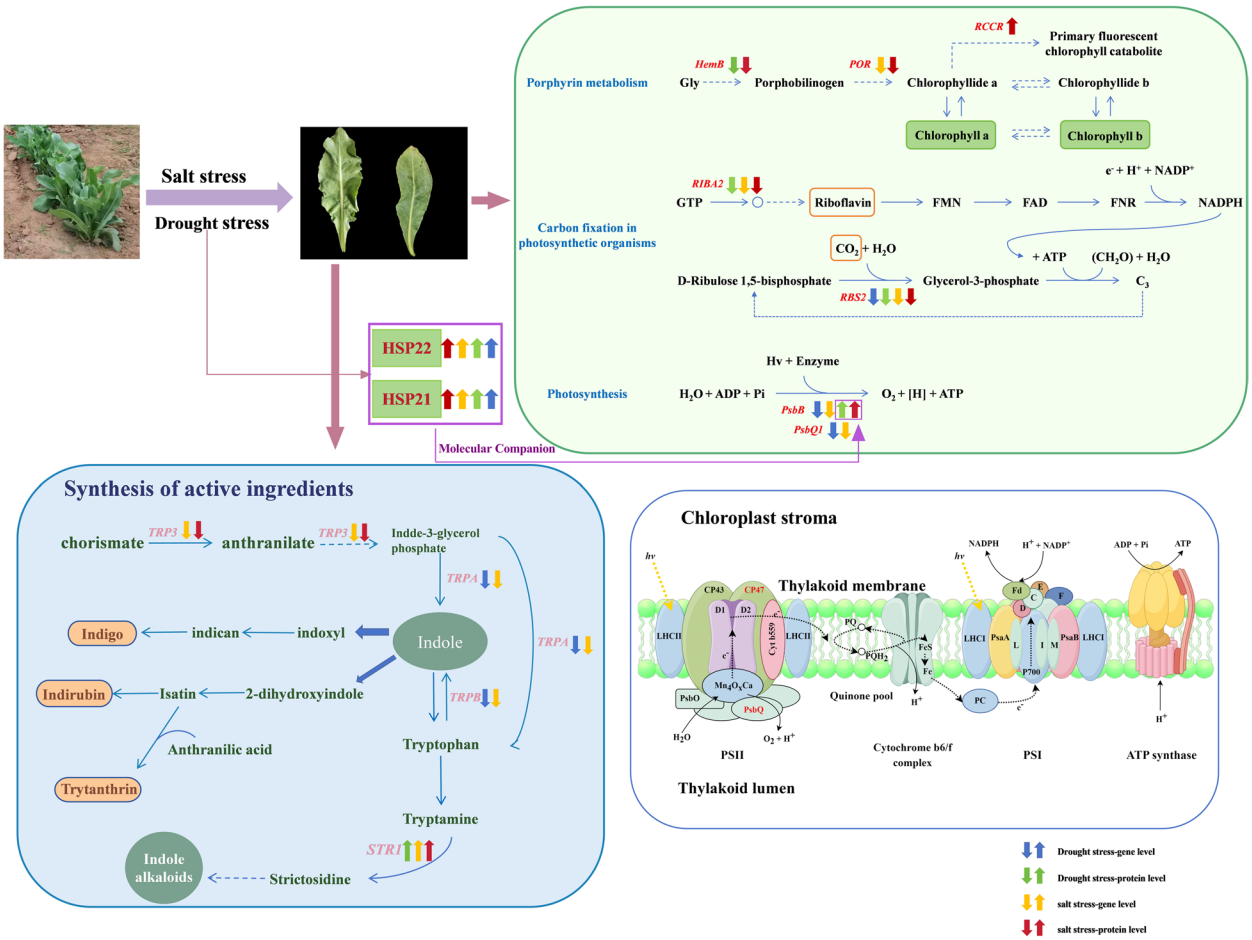

Fig. 13 Model of the regulatory mechanisms underlying the effects of abiotic stresses on the quality of *Isatidis Folium*. The upward and downward arrows behind the genes and proteins represent the up-regulation and down-regulation trend, respectively. Specifically, blue and green arrows represent genes and proteins affected by drought stress, respectively; orange and red arrows represent genes and proteins affected by salt stress, respectively

an evaluation of the effects of salt and drought stresses on the herbal quality of *Isatidis Folium* and their specific regulatory mechanisms based on multi-component quantitative analysis as well as combined proteomic and transcriptomic analysis, which provides a new and valuable scientific idea and research basis for solving the current dilemma of the quality control of *Isatidis Folium*.

Acknowledgements
The authors would like to thank all those who contributed to this study.

Clinical trial number
Not applicable.

Authors' contributions
WZY and CBR were the main contributors performing the entire experimental process and writing the manuscript. DJX and DTT assisted in analyzing and visualizing the results of transcriptomic and proteomic. WRY, CYW, and LX assisted in conducting the multi-component content determination. FJL and PJX provided suggestions for the experimental plan. YMN and HJX were responsible for proposing the research directions and overseeing the entire research process, and they have received funding supports. All authors read and approved the final manuscript.

Funding
This research was funded by the Natural Science Foundation of China (No. 82004212), the Project of Shandong Traditional Chinese Medicine Plan (No. M-2022259), and the Coconstruction Project of the National Administration of Traditional Chinese Medicine (No.GZY-KJS-SD-2023-084).

Data availability
The complete transcriptomic and proteomic data that support the findings of this study have been deposited in the GSA and ProteomeXchange databases, respectively, with the primary accession codes CRA020651 and PXD058215, respectively.

Declarations

Ethics approval and consent to participate
Not applicable.

Consent for publication
Not applicable.

Competing interests
The authors declare no competing interests.

Author details
[1]Department of Clinical Pharmacy, The First Affiliated Hospital of Shandong First Medical University & Shandong Provincial Qianfoshan Hospital, Jinan, China. [2]Biomedical Sciences College & Shandong Medical Biotechnology Research Center, National Health Commission Key Laboratory of Biotechnology Drugs, Shandong First Medical University & Shandong Academy of Medical Sciences, Jinan, China. [3]College of Traditional Chinese Medicine, Shandong University of Traditional Chinese Medicine, Jinan, China. [4]Institute of Traditional Chinese Medicine Pharmacology, Shandong Academy of Chinese Medicine, Jinan, China.

Received: 12 November 2024 Accepted: 26 February 2025
Published online: 14 March 2025

References

1. Chen J, Zhu Z, Gao T, Chen Y, Yang Q, Fu C, Zhu Y, Wang F, Liao W. Isatidis radix and Isatidis Folium: a systematic review on ethnopharmacology, phytochemistry and pharmacology. J Ethnopharmacol. 2022;283: 114648.
2. Commission CP. Chinese pharmacopoeia. Beijing: The Medicine Science and Technology Press of China; 2020.
3. Zhong WG, Xu QH, Meng FD. Research progress of Folium isatidis. Ginseng Research. 2011;23(03):38–41.
4. Deng Y-P, Liu Y-Y, Liu Z, Li J, Zhao L-M, Xiao H, Ding X-H, Yang Z-Q. Antiviral activity of Folium isatidis derived extracts in vitro and in vivo. Am J Chin Med. 2013;41(4):957–69.
5. Wang BX. Experimental study of Chinese herbal medicine against hepatitis b virus. New Chinese Medicine. 2001;02:3–5.
6. Wu B, Wang L, Jiang L, Dong L, Xu F, Lu Y, Jin J, Wang Z, Liang G, Shan X. n-butanol extract from Folium isatidis inhibits the lipopolysaccharide-induced downregulation of CXCR1 and CXCR2 on human neutrophils. Mol Med Rep. 2018;17(1):179–85.
7. Liu SF, Zhang YY, Zhou L, Lin B, Huang XX, Wang XB, Song SJ. Alkaloids with neuroprotective effects from the leaves of Isatis indigotica collected in the Anhui Province, China. Phytochemistry. 2018;149:132–9.
8. Ji ZQ, Li YL, Zhang YF, Shi L. Studies on chemical constituents of Folium Isatidis. China Pharmacist. 2013;16(10):1467–9.
9. Xiong XL, Yuan MM, Wu LF, Li KC, Zhong RJ. Studies on the chemical constituents of Folium isatidis. Journal of Chinese Medicinal Materials. 2022;11:2637–42.
10. Deng X, Gao G, Zheng S, Li F. Qualitative and quantitative analysis of flavonoids in the leaves of Isatis indigatica Fort. by ultra-performance liquid chromatography with PDA and electrospray ionization tandem mass spectrometry detection. J Pharm Biomed Anal. 2008;48(3):562–7.
11. Liu JF, Zhang XM, Xue DQ, Jiang ZY, Gu Q, Chen JJ. Studies on the chemical constituents of Folium isatidis. China J Chin Materia Med. 2006;23:1961–5.
12. Mao XF. Research on extraction and isolation of Folium isatidis'ogranic acids and its acute toxic experiment. Master. Lanzhou: Gansu Agricultural University; 2018.
13. Li XH, Liang JP, Lu XH. Studies on the chemical constituents of Folium isatidis. Shizhen Journal of Traditional Chinese Medicine Research. 2011;22(09):2144–5.
14. Ruan JL, Zou JH, Cai YL. A study on the chemical composition of Folium isatidis. China J Chin Materia Med. 2005;19:49–50.
15. Guo X, Hu XL, Wang YR, Yang ZF, Wang YT, Li ZT, Hu P. Systematic separation, purification and composition analysis of polysaccharides from Isatis indigotica. Journal of Chinese Medicinal Materials. 2016;47(09):1508–14.
16. Bai NN, Wang WX, Li Q, Guo YH, Meng XL, Chen Y. Study and application of isatis indigotica polysaccharide. Botanical Research. 2018;7(3):268–76.
17. Yuan MM, Zhang W, Xiong XL, Zhong RJ, Wu LF. Advances in study of chemical constituents and pharmacological effects of Isatidis Folium. Drug Evaluation. 2022;19(16):1019–22.
18. Lu HT, Liu J, Deng R, Song JY. Preparative isolation and purification of indigo and indirubin from Folium isatidis by high-speed counter-current chromatography. Phytochem Anal. 2012;23(6):637–41.
19. Wu X, Chen X, Jia D, Cao Y, Gao S, Guo Z, Zerbe P, Chai Y, Diao Y, Zhang L. Corrigendum: characterization of anti-leukemia components from Indigo naturalis using comprehensive two-dimensional K562/cell membrane chromatography and in silico target identification. Sci Rep. 2016;6:30103.
20. Spink BC, Hussain MM, Katz BH, Eisele L, Spink DC. Transient induction of cytochromes P450 1A1 and 1B1 in MCF-7 human breast cancer cells by indirubin. Biochem Pharmacol. 2003;66(12):2313–21.
21. Gao GX, Dong Z. Exploration of Chinese medicine quality standardization and modernization development of Chinese medicine. China Medical Herald. 2010;7(02):76–7.
22. Xiao YH, Xia Y, Cheng PP, Fang Y, Da GZ, Huang J, Zhang XQ. Simultaneous determination of indigo and indirubin in Folium isatidis by RP-HPLC. Herald Med. 2015;34(11):1506–8.
23. Wang Y, Qiao CZ, Yin C. Identification of Folium isatidis from different populations by high performance capillary electrophoresis. Chinese Traditional and Herbal Drugs. 2000;07:69–71.
24. Sun Q, Leng J, Tang L, Wang L, Fu C. A comprehensive review of the chemistry, pharmacokinetics, pharmacology, clinical applications, adverse events, and quality control of indigo naturalis. Front Pharmacol. 2021;12: 664022.
25. Yang CF, Kong QY, Sun MJ. An introduction to the progress of the research on Isatidis Folium. Shandong Journal of Animal Science and Veterinary Medicine. 2019;40(05):78–80.
26. Hsieh Y-C, Wu M-S, Lee H-C, Hsieh C-Y, Huang S-S, Tsai C-F, Lin Y-T, Lin M-C, Tseng S-H, Wang D-Y. Development of the species-specific multiplex PCR and DNA sequencing methods for rapid authentication of Isatidis Folium and its adulterants. J Food Drug Anal. 2021;29(2):303–10.
27. Yu Y, Gong D, Zhu Y, Wei W, Sun G. Quality consistency evaluation of Isatidis Folium combined with equal weight quantified ratio fingerprint method and determination of antioxidant activity. J Chromatogr B Analyt Technol Biomed Life Sci. 2018;1095:149–56.
28. Li L, Fan Z, Gan Q, Xiao G, Luan M, Zhu R, Zhang Z. Conservative mechanism through various rapeseed (Brassica napus L.) varieties respond to heavy metal (Cadmium, Lead, Arsenic) stress. Front Plant Sci. 2024;15:1521075.
29. Choudhary R, Ahmad F, Kaya C, Upadhyay SK, Muneer S, Kumar V, Meena M, Liu H, Upadhyaya H, Seth CS. Decrypting proteomics, transcriptomics, genomics, and integrated omics for augmenting the abiotic, biotic, and climate change stress resilience in plants. J Plant Physiol. 2025;305: 154430.
30. Wang D, Li J, Li S, Fu J, Liu B, Cao D. Multi-omics analysis of hexaploid triticale that show molecular responses to salt stress during seed germination. Front Plant Sci. 2024;15:1529961.
31. Wang C, Wu D, Jiang L, Liu X, Xie T. Multi-omics elucidates difference in accumulation of bioactive constituents in licorice (Glycyrrhiza uralensis) under drought stress. Molecules. 2023;28(20):7042.
32. Zhao Q, Dong M, Li M, Jin L, Paré PW. Light-induced flavonoid biosynthesis in Sinopodophyllum hexandrum with high-altitude adaptation. Plants (Basel). 2023;12(3):575.
33. Pan J, Huang C, Yao W, Niu T, Yang X, Wang R. Full-length transcriptome, proteomics and metabolite analysis reveal candidate genes involved triterpenoid saponin biosynthesis in Dipsacus asperoides. Front Plant Sci. 2023;14: 1134352.
34. Wu S, Jia X, Tian B, Zhang F, Zhao J, Xie X, Shan C, Wang H, Guo X, Han J. Physiological and cellular ultrastructural responses of isatis indigotica Fort. under salt stress. Plants (Basel). 2024;13(12):1593.
35. Ma J, Ren W, Jiang S, Kong L, Ma L, He J, Wang D, Liu W, Ma W, Liu X. Identification and expression analysis of the RBOH gene family of Isatis indigotica Fort. and the potential regulation mechanism of RBOH gene on H2O2 under salt stress. Plant Cell Rep. 2025;44(3):52.
36. Wang Y, Zhou RY, Ma LM, Bai Y, Guan JL, Tang XQ. Seed germination and seedling growth responses of Isatis indigotica in five populations from saline environments. Acta Pratacul Sin. 2018;27(07):145–54.
37. Law of the People's Republic of China on Traditional Chinese Medicine. Gazette of the Standing Committee of the National People's Congress of the People's Republic of China. 2017(01):5–11. https://flk.npc.gov.cn/detail2.html?MmM5MDlmZGQ2NzhiZjE3OTAxNjc4YmY4MzgyODA5YWI%3D.
38. Ma YE. Effect of soil moisture content on the growth and physiological characteristics of sphagnum pine seedlings. Journal of Green Science and Technology. 2022;24(23):150–3.

39. Mi YW, Wang GX, Gong CW, Cai ZP, Wu WG. Effect of salt stress on the growth and resistance physiology of young woad seedlings. Acta Pratacul Sin. 2018;27(6):43–51.
40. Song SW. Study on response characteristics of six mulberry varieties under salt stress. Master. Lanzhou: Shandong Agricultural University; 2011.
41. Huang QC, Xu YM, Wei YH, Liang YZ. Comparison of carotenoid content in dark leaf plants. Hubei Agricultural Sciences. 2013;52(11):2573–4.
42. Bradford MM. A rapid and sensitive method for the quantitation of microgram quantities of protein utilizing the principle of protein-dye binding. Anal Biochem. 1976;72:248–54.
43. Wisniewski JR, Zougman A, Nagaraj N, Mann M. Universal sample preparation method for proteome analysis. Nat Methods. 2009;6(5):359–62.
44. Partners C-NMa. Database resources of the National Genomics Data Center, China National Center for Bioinformation in 2022. Nucleic Acids Res. 2022;50(D1):D27-D38.
45. Chen T, Chen X, Zhang S, Zhu J, Tang B, Wang A, Dong L, Zhang Z, Yu C, Sun Y, et al. The genome sequence archive family: toward explosive data growth and diverse data types. Genomics Proteomics Bioinformatics. 2021;19(4):578–83.
46. Ma J, Chen T, Wu S, Yang C, Bai M, Shu K, Li K, Zhang G, Jin Z, He F, et al. iProX: an integrated proteome resource. Nucleic Acids Res. 2019;47(D1):D1211–7.
47. Chen T, Ma J, Liu Y, Chen Z, Xiao N, Lu Y, Fu Y, Yang C, Li M, Wu S, et al. iProX in 2021: connecting proteomics data sharing with big data. Nucleic Acids Res. 2022;50(D1):D1522–7.
48. Lh Y, Dl X. Response and adaptation of plant morphology to drought stress. Hubei Agricultural Sciences. 2019;58(08):5–7.
49. Sun MC, Yin ZP, Ma XL, Zhou LJ, Ren J, Song XS. Effects of salt stress on physiological characteristics and ion contents in Cerasus humilis seedlings. Nonwood Forest Res. 2012;30(02):33–37.
50. Abdelaziz ME, Atia MAM, Abdelsattar M, Abdelaziz SM, Ibrahim TAA, Abdeldaym EA. Unravelling the Role of Piriformospora indica in Combating Water Deficiency by Modulating Physiological Performance and Chlorophyll Metabolism-Related Genes in Cucumis sativus. Horticulturae. 2021;7(10):399.
51. Zhang SW, Heyes DJ, Feng LL, Sun WL, Johannissen LO, Liu HT, Levy CW, Li XM, Yang J, Yu XL, et al. Structural basis for enzymatic photocatalysis in chlorophyll biosynthesis. Nature. 2019;574(7780):722-+.
52. Wang Y, Jia BY, Ren HJ, Feng Z. Ploidy level enhances the photosynthetic capacity of a tetraploid variety of Acer buergerianum Miq. Peerj. 2021;9:9.
53. Tang WJ, Wang WQ, Chen DQ, Ji Q, Jing YJ, Wang HY, Lin RC. Transposase-derived proteins FHY3/FAR1 interact with PHYTOCHROME-INTERACTING FACTOR1 to regulate chlorophyll biosynthesis by modulating HEMB1 during deetiolation in Arabidopsis. Plant Cell. 2012;24(5):1984–2000.
54. Huang WW. Preliminary studies on the regulatory mechanism of photosynthesisduring leaf development in poplar 84K. Master. Beijing: Beijing Forestry University; 2022.
55. Su J, Jiao Q, Jia T, Hu X. The photosystem-II repair cycle: updates and open questions. Planta. 2023;259(1):20.
56. Yamori W, Shikanai T. Physiological functions of cyclic electron transport around photosystem I in sustaining photosynthesis and plant growth. Annu Rev Plant Biol. 2016;67:81.
57. Jin HL, Liu B, Luo LJ, Feng DR, Wang P, Liu J, Da QG, He YM, Qi KB, Wang JF, et al. HYPERSENSITIVE TO HIGH LIGHT1 interacts with LOW QUANTUM YIELD OF PHOTOSYSTEM II1 and functions in protection of photosystem II from photodamage in. Plant Cell. 2014;26(3):1213–29.
58. Yi XP, Hargett SR, Frankel LK, Bricker TM. The PsbQ protein is required in for photosystem II assembly/stability and photoautotrophy under low light conditions. J Biol Chem. 2006;281(36):26260–7.
59. Allahverdiyeva Y, Suorsa M, Rossi F, Pavesi A, Kater MM, Antonacci A, Tadini L, Pribil M, Schneider A, Wanner G, et al. Arabidopsis plants lacking PsbQ and PsbR subunits of the oxygen-evolving complex show altered PSII super-complex organization and short-term adaptive mechanisms. Plant J. 2013;75(4):671–84.
60. Portis AR. Rubisco activase - Rubisco's catalytic chaperone. Photosynth Res. 2003;75(1):11–27.
61. Gionfriddo M, Zang K, Hayer-Hartl M. The challenge of engineering Rubisco for improving photosynthesis. FEBS Lett. 2023;597(13):1679–80.
62. Chen HM, Chen Y, Wang D, Jiang DA. The role of ribulose-1,5-bisphosphate carboxylase/oxygenase activase in resistance of plant to abiotic stresses. Plant Physiology Journal. 2016;52(11):1637–48.
63. Li SY, Du L, Bernhardt R. Redox partners: function modulators of bacterial P450 enzymes. Trends Microbiol. 2020;28(6):445–54.
64. Iyanagi T. Roles of ferredoxin-NADP oxidoreductase and flavodoxin in NAD(P)H-dependent electron transfer systems. Antioxidants (Basel). 2022;11(11):2143.
65. Utschig LM, Brahmachari U, Mulfort KL, Niklas J, Poluektov OG. Biohybrid photosynthetic charge accumulation detected by flavin semiquinone formation in ferredoxin-NADP reductase. Chem Sci. 2022;13(22):6502–11.
66. Aghaie P, Tafreshi SAH. Central role of 70-kDa heat shock protein in adaptation of plants to drought stress. Cell Stress Chaperon. 2020;25(6):1071–81.
67. Kang Y, Lee K, Hoshikawa K, Kang M, Jang S. Molecular bases of heat stress responses in vegetable crops with focusing on heat shock factors and heat shock proteins. Frontiers in Plant Science. 2022;13:837152.
68. Waters ER, Vierling E. Plant small heat shock proteins - evolutionary and functional diversity. New Phytol. 2020;227(1):24–37.
69. Kim DH, Xu ZY, Hwang I. AtHSP17.8 overexpression in transgenic lettuce gives rise to dehydration and salt stress resistance phenotypes through modulation of ABA-mediated signaling. Plant Cell Rep. 2013;32(12):1953–63.
70. Ramakrishna G, Singh A, Kaur P, Yadav SS, Sharma S, Gaikwad K. Genome wide identification and characterization of small heat shock protein gene family in pigeonpea and their expression profiling during abiotic stress conditions. Int J Biol Macromol. 2022;197:88–102.
71. Huther CM, Ramm A, Rombaldi CV, Bacarin MA. Physiological response to heat stress of tomato "Micro-Tom" plants expressing high and low levels of mitochondrial sHSP23.6 protein. Plant Growth Regul. 2013;70(2):175–85.
72. Neta-Sharir I, Isaacson T, Lurie S, Weiss D. Dual role for tomato heat shock protein 21: protecting photosystem II from oxidative stress and promoting color changes during fruit maturation. Plant Cell. 2005;17(6):1829–38.
73. Pan XX, Zheng Y, Lei KR, Tao WL, Zhou N. Systematic analysis of Heat Shock Protein 70 (HSP70) gene family in radish and potential roles in stress tolerance. BMC Plant Biol. 2024;24(1):2.
74. Liu J, Pang X, Cheng Y, Yin YH, Zhang Q, Su WB, Hu B, Guo QW, Ha S, Zhang JP, et al. The Hsp70 Gene Family in Solanum tuberosum: Genome-Wide Identification, Phylogeny, and Expression Patterns. Sci Rep-Uk. 2018;8(1):16628.
75. Li YY, Zhang ZR, Di ZX, Qi XY, Zhang Y, Wang C, Lu YZ, Zheng J. Genome-wide investigation of heat shock protein 70 gene family in sorbus pohuashanensis and their expression analysis in response to abiotic stresses. Genomics and Applied Biology. 2022;41(Z1):1973–84.
76. Fan C, Yang J, Chen R, Liu W, Xiang X. Identification and expression analysis of the HSP70 gene family under abiotic stresses in Litchi chinensis. Chin J Biotechnol. 2024;40(04):1102–19.
77. Hua YJ, Wang SN, Liu ZX, Liu XH, Zou LS, Gu W, Hou Y, Ma Y, Luo YY, Liu JX. iTRAQ-based quantitative proteomic analysis of cultivated and its wild-type. J Proteomics. 2016;139:13–25.
78. Chompa SS, Zuan ATK, Amin AM, Hun TG, Ghazali AHA, Sadeq BM, Akter A, Rahman ME, Rashid HO. Growth and protein response of rice plant with plant growth-promoting rhizobacteria inoculations under salt stress conditions. Int Microbiol. 2024;27(4):1151–68.
79. Zhi QQ, Chen Y, Hu H, Huang WQ, Bao GG, Wan XR. Physiological and transcriptome analyses reveal tissue-specific responses of Leucaena plants to drought stress. Plant Physiol Bioch. 2024;214:214.
80. Lee S, Lee DW, Lee Y, Mayer U, Stierhof YD, Lee S, Jürgens G, Hwang I. Heat shock protein cognate 70–4 and an E3 ubiquitin ligase, CHIP, mediate plastid-destined precursor degradation through the ubiquitin-26S proteasome system in. Plant Cell. 2009;21(12):3984–4001.
81. Lin WJ, Huang W, Ning SJ, Wang XH, Ye Q, Wei D. De novo characterization of the Baphicacanthus cusia(Nees) Bremek transcriptome and analysis of candidate genes involved in indican biosynthesis and metabolism. Plos One. 2018;13(7):0199788.
82. Inoue S, Morita R, Minami Y. An indigo-producing plant, Polygonum tinctorium, possesses a flavin-containing monooxygenase capable of oxidizing indole. Biochem Bioph Res Co. 2021;543:95–95.

83. Guo ZY, Chen JF, Lv ZY, Huang YX, Tan HX, Zhang L, Diao Y. Molecular cloning and functional characterization of BcTSA in the biosynthesis of indole alkaloids in. Frontiers in Plant Science. 2023;14:1174582.
84. Warzecha H, Frank A, Peer M, Gillam EMJ, Guengerich FP, Unger M. Formation of the indigo precursor indican in genetically engineered tobacco plants and cell cultures. Plant Biotechnol J. 2007;5(1):185–91.
85. Zhang YM, Su Y, Dai ZW, Lu M, Sun W, Yang W, Wu SS, Wan ZT, Wan HH, Zhai JW. Integration of the metabolome and transcriptome reveals indigo biosynthesis in flowers under freezing treatment. Peerj. 2022;10:10.
86. Chen TT, Wang XN, Zhuang L, Shao AL, Lu YH, Zhang HR. Development and optimization of a microbial co-culture system for heterologous indigo biosynthesis. Microb Cell Fact. 2021;20(1):154.
87. Chen JF, Li Q, Wang Y, Zhang QL, Zhang L, Chen WS. Comprehensive transcriptomic profiling of Isatis indigotica leaves reveals biosynthesis of indole active ingredients. Sci Sinica Vitae. 2018;48(04):412–22.
88. Kim J, Lee J, Lee PG, Kim EJ, Kroutil W, Kim BG. Elucidating cysteine-assisted synthesis of indirubin by a Flavin-containing monooxygenase. Acs Catal. 2019;9(10):9539–44.
89. Liao W, Song J, Han L, Zhang DK. Research progress of natural product tryptanthrin. Nat Prod Res Dev. 2023;35(11):2003–13.
90. Hwang MG, Kim K, Lee WK, Cho MH. AtTBP2 and AtTRP2 in Arabidopsis encode proteins that bind plant telomeric DNA and induce DNA bending in vitro. Mol Genet Genomics. 2005;273(1):66–75.
91. Jian OY, Shao X, Li JY. Indole-3-glycerol phosphate, a branchpoint of indole-3-acetic acid biosynthesis from the tryptophan biosynthetic pathway in. Plant J. 2000;24(3):327–33.
92. Zhao JJ. Enzymatic properties and structural analysis of α and β subunits of tryptophan synthase in Mycobacterium tuberculosis H37Rv. Master. Shanghai: Fudan University; 2008.
93. Wang M, Li QR. Transient expression of strictosidine synthase in tobacco leaves by vacuum infiltration. Acta Biochim Biophys Sin. 2002;06:703–6.

Publisher's Note